I.O.S.

CURRENTS, DISPERSION AND LIGHT TRANSMITTANCE MEASUREMENTS ON THE MADEIRA ABYSSAL PLAIN

FINAL REPORT MARCH 1987

BY

P.M. SAUNDERS

REPORT NO. 241

1987

OCEAN DISPOSAL OF HIGH LEVEL RADIOACTIVE WASTE

A RESEARCH REPORT PREPARED FOR THE

DEPARTMENT OF THE ENVIRONMENT

INSTITUTE OF
OCEANOGRAPHIC SCIENCES
DEACON LABORATORY

NATURAL ENVIRONMENT RESEARCH COUNCIL

INSTITUTE OF OCEANOGRAPHIC SCIENCES

DEACON LABORATORY

Wormley, Godalming,
Surrey, GU8 5UB, U.K.

Telephone: 0428 79 4141
Telex: 858833 OCEANS G
Telefax: 0428 79 3066

Director: Dr. A.S. Laughton FRS

Natural Environment Research Council

INSTITUTE OF OCEANOGRAPHIC SCIENCES

DEACON LABORATORY

REPORT No. 241

Currents, dispersion and light transmittance measurements on the Madeira Abyssal Plain

Final Report March 1987

by

P.M. Saunders

1987

DOCUMENT DATA SHEET

AUTHOR	SAUNDERS, P.M.	*PUBLICATION DATE* 1987
TITLE	Currents, dispersion and light transmittance measurements on the Madeira Abyssal Plain. Final Report March 1987.	
REFERENCE	Institute of Oceanographic Sciences, Deacon Laboratory, Report, No. 241, 55pp.	

ABSTRACT

Near bottom currents have been measured in the GME study area (near 31 30N 25W) over a 3 year period. The sites selected were on top of a small abyssal hill, on its flank and 30km distant from it on the abyssal plain. The magnitude of the mean currents 10m above the seabed at the three sites was 1-2 cm/s but their directions were quite different reflecting the presence of a clockwise vortex trapped over the hill.

The variability of the currents is examined: for periods greater than 120 days the variance is concentrated in the east component, and for periods 50-120 days the variance is concentrated in the north component. From estimates of the integral time scale of these motions (6-14 days) horizontal diffusivities of between 2 and 5 x 10^2 m^2s^{-1} have been deduced.

Light transmittance measurements have been made from lowerings within the Canary Basin and evidence for resuspended sediment is found at most sites. Measurements of light transmittance were also made for about 1 year and 3m above the bottom at the GME study site: fluctuations were small, corresponded to a particle concentration increase of only a factor of 3, and were uncorrelated with current speeds.

Currents in excess of 10 cm/s occurred infrequently on the plain (about 0.3% of the time) but four times as frequently on and around the hill. Estimates of the highest speeds achieved on average every 50 years have been derived and found less than 20 cm/s. This value is a conservative estimate of the critical speed required to erode the sediment. Thus very infrequent erosion around GME and especially on the hills can not be excluded.

ISSUING ORGANISATION	Institute of Oceanographic Sciences Deacon Laboratory Wormley, Godalming Surrey GU8 5UB. UK. Director: Dr A S Laughton FRS	*TELEPHONE* 0428 79 4141 *TELEX* 858833 OCEANS G *TELEFAX* 0428 79 3066

KEYWORDS	*BOTTOM CURRENTS* *BOTTOM TOPOGRAPHY EFFECTS* *LIGHT TRANSMISSION* *RESUSPENDED SEDIMENTS* *GREAT METEOR EAST* *MADEIRA ABYSSAL PLAIN*	*CONTRACT* PECD7/9 /216 *PROJECT* PH21 *PRICE* £16.00

Copies of this report are available from:
The Library, Institute of Oceanographic Sciences, Deacon Laboratory.

CONTENTS **Page**

INTRODUCTION

Measurements of currents near the sea-bed in the very deep parts of the N.E. Atlantic Ocean have been carried out in the last two decades by a number of European laboratories. A summary reveals the very weak nature of the abyssal circulation[1]. Under contract to the Department of the Environment which ended in 1984 IOS carried out some of these measurements using moored current meters and drifting neutrally buoyant floats and reported their work[2].

A new programme of measurement within the water column was started in 1984. This included observations of currents at a specific location (GME, the Great Meteor East study site) employing moored current meters, and measurements of dispersion using a group of neutrally buoyant floats free drifting at a depth of 3000m and tracked from acoustic listening stations. Both programmes were to last 2 years and because of an early start the moored current measurements, which are reported here, lasted nearly 3 years.

The purpose of the measurements at GME was threefold:-

(1) to establish the climatology of currents on the abyssal plain and their dispersion

(2) to observe the effect of a neighbouring 400m-high hill on these currents and their dispersion, and

(3) to document the occurrence of strong current in the area and to determine whether they were capable of eroding the sea bed and carrying sediment considerable distances.

In addition to the above, hydrographic observations were made when the ship was on site by lowering an instrument (CTD) which recorded pressure (depth), temperature, conductivity (salinity), dissolved oxygen and light transmittance. The last variable, transmittance, measures the clarity of the water and provides an estimate of the mass of sediment in the water.

THE SITE FOR MEASUREMENTS

The Great Meteor East study site, a 100km box centred on 31 30N 25 00W, lies in the Madeira abyssal plain in the centre of the Canary basin. To the west of GME the abyssal plain abuts against the lower flank of the Mid-Atlantic Ridge, and is

characterised by the outcropping of abyssal hills elongated in the SW-NE direction[3]. To the east of GME the abyssal plain merges smoothly into the deepest parts of the lower continental rise and to the north the basin is bounded by the Azores-Gibraltar rise. The local and regional bathymetry is shown in Figure 1. At GME the water depth on the abyssal plain is approximately 5440m and an unnamed abyssal hill at 31 30N, 25 10W has a minimum depth of just less than 5000m and hence a height of 450m above the plain.

Three sites were selected for long-term current measurements:-

(i) on the plain about 30km from the nearest hill and representative of the abyssal plain
(ii) on the summit of the small hill
(iii) at the foot of the same hill,

the last two to determine the effect of the hill on the flow. Care had to be exercised in the selection of these sites since they would be occupied by instrumentation for a period within which other scientists at IOS were investigating GME. A short duration current measurement was also made in the 10km x 10km region centred on 31 17N 25 24W.

Our experience at other locations[2] suggested that currents should be measured near to the sea-bed and about 1000m above it, the latter in order to establish the penetration of bottom currents (upwards) in the water column. A third instrument at 100m above bottom was made part of the mooring design primarily for redundancy. Thus three moorings were deployed, one at each of the above sites, with three instruments on each (Fig.2). Such moorings have a safe lifetime of about 1 year so 3 deployments were made to cover the nearly 3 year period from 30 January 1984 to 24 September 1986.

INSTRUMENTATION, MOORINGS AND DATA QUALITY

The data described in this report were gathered from Aanderaa RCM5 current meters. Instruments are individually calibrated for rotor speed, compass direction and temperature. The rotor stall speed lies between 1.5 and 2.0cm s^{-1} and direction values are reproducible in pre-deployment and post-calibrations to ±3°. The temperature circuit has been modified[4] to give a sensitivity of .0025°C per count.

Moorings were of 10mm and 12mm braided polypropylene with 3000kg of chain anchor and 6 17" diameter Benthos glass spheres which provided about 150kg of buoyancy; acoustic releases were of IOS design. The weak currents measured ensured that mooring knock-down was negligible (<10m).

Moorings were first laid on Discovery Cruise 144 (January/February 1984) and recovered on Darwin Cruise 1/85 (February 1985); the second deployment laid on Darwin 1/85 was recovered on Darwin Cruise 9A/85 (November 1985): the third deployment laid on Darwin 9A/85 was recovered on Discovery Cruise 162 (September 1986). Details concerning the moorings are shown in table 1 and concerning the current meters are shown in table 2.

The data recovery record was impaired by the loss of mooring 399 which we suppose had pre-released, surfaced and drifted away. In all 28 instruments were deployed for an expected duration of 8770 days but only 7346 or 84% of the data were recovered. The temperature records were more disappointing in part due to ageing instrumentation and in part due to faulty batteries suplied by the manufacturer to which the temperature measurements were particularly sensitive.

TABLE 1

Mooring locations

Site	Mooring	Latitude, °N	Longitude, °W	Depth, m
PLAIN	365	31 31.3	24 45.4	5438
	391	31 30.2	24 45.2	5438
	400	31 28.8	24 43.8	5444
HILL-FOOT	366	31 31.1	25 01.1	5398
	389	31 30.4	25 03.1	5433
	399*	31 32.4	25 01.0	5444
HILL-TOP	367	31 29.7	25 09.6	4999
	387	31 29.2	25 08.4	4989
	401	31 29.4	25 08.5	5055
GMEBOX	-	31 14.9	25 26.6	5450

*Mooring not (yet) recovered

TABLE 2

Duration and Quality of Current Data

Site	Deploy.	Ident.	Depth	Start	End	Duration	Quality
	1	36501	4343	30-I-84	23-II-85	390	OK
P		36502	5334	"	"	390	OK
L		36503	5428	"	"	390	OK
A	2	39101	4347	27-II-85	5-X-85	220	Short
I		39102	5333	"	18-XI-85	264	No temp.
N		39103	5427	"	"	264	OK
	3	40004	4368	19-XI-85	24-IX-86	309	OK
		40005	5342	"	"	309	Temp. only 135 days
		40006	5435	"	"	309	OK
H	1	36601	4307	5-II-84	23-II-85	384	No vane, no temp.
I		36602	5295	"	"	384	OK
L		36603	5388	"	11-I-85	341	Short
L / F	2	38901	4341	24-II-85	18-XI-85	267	OK
		38902	5327	"	"	267	OK
O		38903	5422	"	20-VI-85	116	Short, no temp.
O	3	39901	4340			0)	
T		39902	5330			0)	Not recovered
		39903	5434			0)	
H	1	36701	3907	6-II-84	5-XII-84	303	Short
I		36702	4906	"	23-II-85	384	No temp.
L		36703	4989	"	"	384	OK
L / T	2	38701	3900	24-II-85	18-XI-85	267	OK
		38702	4882	"	"	267	OK
O		38703	4978	"	"	267	OK
P	3	40101	3962	20-XI-85	27-XI-85	8	Fails
		40102	4956	"	24-IX-86	309	Temp. only 265 days
		40103	5046	"	"	309	OK
GME BOX	2	-	5447	19-VII-85	19-XI-85	122	With camera

DATA PROCESSING

Data were translated from 1/4" field tape to 1/2" computer compatible magnetic tape using a reader of IOS construction and a HP2100 computer. Subsequent processing and archiving of data was carried out on the NERC Honeywell 66/DPS 300 at Bidston.

Data were first checked for time-base errors; reconcilation was always possible after partial or repeated data cycles were recognised. Rotor count was converted to rotor speed using the expression

$$s = a\Omega + b$$

where Ω is the number of revolutions/second and s is the current in cm/s: $a = 46 \pm 1$ and $b = 1.8 \pm 3$. Temperature was obtained from a similar linear equation[4] and direction was converted from one of its 1024 possible values using a look-up table constructed from 20 calibration values. The correction for magnetic deviation at the field site was also made (13°W).

Temperature and direction measurements are made on the hour, and speed is the average for the hour preceding. To take account of these differences, pairs of direction and temperature values are averaged and associated with the intervening speed and all assigned a mid-hour time. Deployment and recovery transients are removed at the beginning and end of the series and outliers (bad data) replaced by absent data values. Providing data gaps are of short duration missing values can subsequently be interpolated.

Because of the very weak currents encountered at abyssal depths the rotor is commonly stalled (10-60 per cent of the time). It is IOS practice to set the current speed equal to the stall value at this time (1.5cm/s): experience shows that the difference resulting from this practice and setting the value equal to zero is very small. Most important conclusions result from the energetic events (strong currents) for which the very weak current treatment is irrelevant.

THE INTERACTION OF THE ABYSSAL HILL WITH THE FLOW

The mean currents at heights 10m and 1000m above the sea-bed at each of the three sites are drawn in table 3: they have a magnitude of between 0 and 2 cm/s and in the lowest 100m quite different directions at the three sites (Fig.3). On the

PLAIN the mean flow is west, at the HILL-FOOT it is south and on the HILL-TOP east; because the 10m and 100m results are so similar we do not display both. These measurements confirm the weakness of the abyssal mean flow in the GME area. (It may be helpful to recall that 1 cm/s ≡ 1 km/day.)

TABLE 3

Experiment mean currents

Site	height above bottom m	mean east cm/s	mean north cm/s	speed cm/s	direction °T	duration days
PLAIN	1000m	**-0.71**	-0.16	0.73	257	919
	10m	**-0.80**	-0.02	0.80	268	963
HILL-FOOT	1000m	-0.04	-0.82	0.82	183	267
	100m	-0.49	**-1.97**	2.03	194	651
HILL-TOP	1000m	-0.05	-0.12	0.12	207	570
	10m	**1.34**	-0.19	1.35	098	960

Components which are bold are reliable: see text.

The above means are derived from the individual instrumental records from each of the deployments: data reports have already been published for the first two deployments[5,6] and a data summary is to be found in tables 9 and 10 at the end of this document.

The reliability of the above component mean values is assessed from the approximate expression[7]

$$\varepsilon^2 = \frac{2\sigma^2 I}{T}$$

σ^2 is the variance of the east/north component about the mean, T is the record duration and I is the Integral time scale. The computation of integral time scale[8] is described in the section on current dispersion (p17 et seq.); here we shall assume a value of 10 days. Given $\sigma \approx 2.5$cm/s for record durations of 250, 650 and 950 days the errors are 0.7cm/s, 0.45cm/s, 0.35cm/s. In table 3 the components printed BOLD are larger than the error estimates given above.

The unreliability of the estimates of the means arises from the uunsteadiness of the currents (reflected in the value of σ) which with finite records leads to sampling errors[7]. The unsteadiness of the currents is readily illustrated (Figs.4-6) by calculating the virtual displacement resulting from an integration of the current. Figure 4 shows the 10m currents on the PLAIN, the most unsteady of the three with long periods (50 days) of flow reversal. Figure 5 shows 100m currents at the HILL-FOOT; whilst the mean direction closely parallels the nearby contours (Fig.3) there are numerous periods of both off-hill and up-hill flow. Figure 6 shows 10m currents on the HILL-TOP; there are periods of near stagnation with bursts of strong easterly flow. The estimates of error however reveal that these directional differences are highly significant.

The explanation for the different mean current direction is to be sought, we believe, in the presence of the abyssal hill itself. Two experiments have been performed in the deep ocean to study the influence of an abyssal hill on the nearby circulation[9,10]. In interpreting the measurements both theoretical[11] and numerical[12] studies have proved very valuable.

The theoretical results predict that vertical uplifting of the sea-water over the abyssal hill will result in a temperature lower than that over the plain at the same pressure. Because of the colder (denser) water there, pressure over the hill is higher giving rise to an anticyclonic circulation; these effects decay exponentially with height. In circumstances, which we determine are met here, the water becomes trapped[11] in the anticyclonic vortex over the hill. If the flow is imagined composed of an oncoming (uniform) stream and the vortex over the hill, then an asymmetric circulation results which is intense on the LHS of the hill looking downstream and weakened on the RHS (Fig.7). Ahead of the hill the flow is deflected to the left, and in the rear to the right, again looking downstream. The rotation of the earth provides the asymmetry so that in the southern hemisphere a mirror image of the above pattern results.

The anticyclonic circulation over the hill has been observed both directly[10] and indirectly by the presence of the dome of cold water[10,11]. The asymmetry on the flanks of the hill, acceleration on the left, deceleration on the right, is also seen[11]. The measurements made at GME further confirm this picture: the cold dome is seen in a lowered CTD section (Fig.8). The flow is, as we have demonstrated, not steady as strictly required by the theory. Nevertheless if the

flow persists for long enough in a certain direction then the above results will hold. Fifty days persistent unidirectional flow should suffice: fluid particles will travel distances of 50-150km in this time which is much larger than the scale of hill (10km). Accordingly we have selected 6 such periods of 'steady' flow as seen by the 10m record on the PLAIN. For the last 25 days of these selected periods the current vectors hve been plotted (Fig.9) at all the sites. When the flow on the plain is westward, note the deflection to the left (south) ahead of the hill and the weak flow on the hill top. When the flow on the plain is to the south (north) note the acceleration (deceleration) on the left (right) flank of the hill. Finally when the flow on the plain is eastward note the intense acceleration on the left flank of the hill and the westward flow south of the hill.

The explanation for mean flow at the three sites now becomes evident. The westward flow on the plain is the flow undisturbed by the effect of the topography; the two other long-term sites both reveal the swirling anticyclonic flow over the hill. The 'hill-top' site lies north of the highest point of the hill (Fig.3): its eastward mean is substantially derived from the intense bursts which accompany the eastward flow on the plain. Such intense flow is not seen 1000m above the seamount and the mean there cannot be distinguished from zero.

THE MEAN FLOW ON THE PLAIN

Away from topography the flow on the plain is found to be westward. The northward component is small and can not be distinguished from zero but the east component is -0.8, -0.8, -0.9 ±.35cm/s at heights of 1000m, 100m and 10m above the sea-bed.

A persistent flux of water at depths between 4000 and 5000m has been measured to pass from the Madeira basin into the Iberian basin to the north[12]. The flow passes through Discovery Gap (Fig.1) and its magnitude ~5 x $10^5 m^3$ is such that if the same flux crossed the latitude 31°N between Madeira and Great Meteor Seamount UNIFORMLY, the northward drift would be less than 1mm/s and hence unobservable. However there is evidence[12] that the flow is concentrated on the east margin of the basin, viz west of Madeira, and is fed either from the south or west. The observation at GME of a westward current suggests the flow on the margin must be fed from the south.

An alternative estimate of the abyssal flow has been derived from the analysis of 10 CTD stations in the form of a triangle of side 500km. The stations were made in the summer of 1983, six months before the current measurements at GME commenced. On the very large scale of the CTD measurements it is supposed that changes are very slow, and the 3 years of current measurements show no evidence of secular change, even locally. The mean current profile is derived using the geostrophic relation along with estimates of the error (see Fig.10). The indeterminacy of the origin of the profile has been removed in two ways[14,15] which are described in the reference cited[13]. Here we shall merely note that both methods strive to ensure that (at each level considered)

(1) the 3 dimensional current vector lies on the density surface, and
(2) north-south components of the flow conserve potential vorticity.

Both solutions predict an eastward component of the flow at all levels with absolute minimum currents near 2500db. The near bottom velocity is ENE, slightly less than 1cm/s, using both techniques. The method averages the result for the region covered by the stations, which is centred near 33 00N 23 30W, and GME lies at its western margin. The diametrically opposite nature of the flow derived by measurement and inference can be attributed to differences in location and scale or a breakdown in the assumptions by which flow is derived from the CTD station data. Unfortunately we are not able to distinguish amongst them.

VARIABILITY OF THE CURRENTS

An examination of any section of the 1 hour data reveals the unmistakable presence of the semi-diurnal tide (period ~12 hours). The principal lunar tidal amplitude M_2 is approximately 3cm/s and the principal solar tidal amplitude S_2 is approximately 1cm/s; their 'beating' gives rise to the familiar Spring-Neap cycle. A third semi-diurnal tidal current N_2 (larger lunar elliptic) also has an amplitude of about 1cm/s. Details of the analysis of these tidal currents will be found in published reports[5,6]; the observations closely conform to the predictions of a barotropic model[16].

For further dicussion of the variability of the currents we shall exclude tides by low pass filtering the data: 24 hour average currents are hereinafter regarded as the data source. The variance of the east and north components of the currents 10m and 1000m above bottom at each site is shown in table 4.

TABLE 4

Variance of low-passed currents at GME, cm^2s^{-2}

Ht. above bottom, m		PLAIN	HILL-FOOT	HILL-TOP
10m	East	4.28	3.18	3.64
		(3)	(2)	(3)
	North	4.14	3.90	1.77
1000m	East	2.76	3.71	3.12
		(3)	(1)	(2)
	North	2.74	2.71	2.04

Numbers in parentheses refer to number of successful deployments

On the plain the variance is equal in the two components, viz is isotropic, and decreases with height above the sea-bed. At 10m on the flank of the hill the variance of the east component is slightly reduced and on the hill-top the north component is considerably reduced. These directions represent the 'uphill' components at the two sites. Finally on the hill top there is little change in variance with height above sea-bed in contrast to the behaviour on the plain.

Further distinctions are seen when the variance is separated into frequency bands by spectral analysis (Figs.11,12) where a variance preserving presentation is employed. For the east component at both the plain and on the hill-top most of the energy is contained in the lowest band of frequencies (127-500 days). For the north component there is more variance in the second and third spectral bands (49-127 days) at both sites. Note that both of these assertions are independent of height: note also the diminished variance in the north component 10m above the sea-bed on the hill-top. The difference in the frequency content of the east and north components is quite evident in a plot of them (Fig.13); the dominant frequency in the east component, at least on the basis of a few cycles, is NOT annual and this confirms a previous finding[1].

Although the variance on the plain has earlier been described as isotropic, a quite different picture emerges if the variance is resolved by frequency interval (Fig.14). For periods in the interval 127-500 days the current 'ellipse' is oriented east west reflecting the excess of east variance over north. For intervals 71-127 days and 49-71 days the current 'ellipse' is oriented

north-south reflecting the excess of north variance over east. In total these three bands contain about 85% of all the low-passed variance.

The above characteristics are suggestive of waves rather than eddies as a description of the current variability and this view is further supported by our estimates of the propagation of signals between the sites. First we examine the coherence between the currents on the plain on the same mooring, viz at 10m and 1000m above bottom. Coherence falls from very near unity at the longest periods to near zero at period of two days. The coherence is about 0.5 at a period of 7 days. The phase lag can not be distinguished from zero. (To estimate coherence errors we have used standard tables and to estimate phase errors we have used approximate expressions attributed to Jenkins[17].) Thus current changes arrive simultaneously at the levels 10m and 1000m above the plain.

Coherence has also been estimated between currents at the sites on the plain and on the hill-top (at 10m height). Coherence magnitude falls to 0.5 at about 30 days period and the phase lag is non-zero for all coherences which differ significantly from zero. The phase is always negative implying the westward propagation of current change. From the phase angle frequency and separation, phase speed can be calculated. Phase speed varies from about 1-8cm/s increasing with decreasing period. Westward propagation and rectilinear current oscillation is a familiar property of planetary or Rossby waves. The minimum phase speed of linear planetary waves in a stratified uniform-depth ocean for the same periods range between 0.6 and 15 cm/s. For periods less than 70 days the observed phase speed is less than the minimum and hence such disturbances are not of the Rossby wave character. Oscillations at longer periods are consistent with Rossby waves, although the orientation of the current ellipse for the first frequency interval suggest a nearly north-south propagating wave whose westward phase speed is no more than the minimum of 0.6cm/s and has a wavelength of about 600km. An explanation in terms of single plane wave is however unsatisfactory[18] and an analysis in terms of a pair of superposed waves is superior, though not attempted here.

HORIZONTAL DISPERSION AT GME

The rate of mixing of a tracer by the fluctuating currents discussed in the previous section is determined by the energy of the flow and its integral time

scale[8]. The latter quantity I_L is given by

$$I_L = \int_0^\infty C(\tau).d\tau$$

where $C(\tau)$ is the correlation function for a velocity component. As has been described elsewhere[2] the correlation function is 'estimated' from current meter data so that diffusivity in the x,y direction is given by

$$K_x, K_y \simeq I_E(u^2, v^2)$$

where u^2, v^2 are the variance in the x,y directions.

The correlation function $\frac{\overline{u(t).u(t+\tau)}}{u^2}$ can be estimated directly from the data or by Fourier transform of the spectrum (Figs.11,12). The author favours fitting a damped cosine for the correlation function, viz

$$C(\tau) = \cos\Omega\tau.\exp - \lambda t$$

$$\text{giving } I = \frac{\lambda}{\Omega^2 + \lambda^2}$$

This form for the correlation function implies a normalised spectral density given by

$$E(f) = 2\lambda\left[\frac{1}{\lambda^2 + (\Omega + 2\pi f)^2} + \frac{1}{\lambda^2 + (\Omega - 2\pi f)^2}\right]$$

where f is cyclic frequency. Whether the expression for $C(\tau)$ or $E(f)$ is employed there are two disposable constants λ, Ω to fit the data.

Fitting the spectral density, Figs.11 and 12, for the plain gives for the east component $2\pi/\Omega$ = 200 days, $1/\lambda$ = 50 days whence I = 14 days. For the north component $2\pi/\Omega$ = 95 days, $1/\lambda$ = 35 days whence I = 6 days. A similar fit of the spectral density exists for the east component of the hill-top data, but the north component is larger, $2\pi/\Omega$ = 200, $1/\lambda$ = 15, I = 12. Combining these estimates of integral time scales with the variance from table 4 gives horizontal (isopycnal) diffusivity values found in table 5.

TABLE 5

Horizontal (isopycnal) diffusion by eddies (10m above sea bed)

Site	Component	Integral time scale, days	variance cm^2s^{-2}	Diffusivity $10^2\ m^2s^{-1}$
PLAIN	E	14 ± 3	4.3	5.2
	N	6 ± 2	4.1	2.1
HILL-TOP	E	14 ± 3	3.6	4.3
	N	12 ± 3	1.8	1.9

On the plain the diffusivities 1000m above the sea-bed are approximately 70% of the values at 10m, and on the hill-top they are quite similar. The values tabulated here are between a factor of two and four higher than diffusivities previously reported[2] on the abyssal plain. Consequently at this rate diffusion is likely to disperse a tracer over a basin, 1000km on a side, in 5-10 years rather than 20 years derived earlier[2]. It will be noted that the hill-top values are indistinguishable from those for the plain. Probably abyssal hills have a larger impact on the vertical (diapycnal) diffusivity augmenting it in the flow separation processes which occur in the lee of the hill.

TRANSMITTANCE MEASUREMENTS IN THE MADEIRA BASIN

Light-scattering measurements have routinely been made from a transmissometer lowered on a conducting wire along with the Neil Brown CTD. The transmissometer, manufactured by Sea-Tech Inc., measures the fraction of light transmitted by a 1m path of sea water: the source is a light-emitting diode with peak wavelength of 660nm[19]. The trace of a typical profile from the Madeira basin in 5000m of water is shown in figure 15. Near the surface living organisms reduce the transmittance to 40-65% and below the depth of light penetration their abundance decreases and transmittance increases sharply. At mid-depth the scattering is principally due to detritus: transmittance continues to increase because of particle decomposition and dissolution but much more slowly. The clearest water is generally found 500-1000m above the bottom with a transmittance value of about 68.5%. Below this depth transmittance decreases generally reaching a second minimum at the bottom of the lowering. The increase near the bottom is attributed to resuspension of sediment from the sea-bed and is the topic under consideration in this and the following section.

In presenting plots of transmittance versus pressure (depth) minor corrections to the instrument voltage are made[20]. The largest correction takes account of the increasing density of sea-water with increasing pressure which increases the mass of sea-water in the 1m path. Accordingly potential transmittance is computed, the transmittance that a sample of sea-water would have if reduced to sea-level pressure at constant salinity and temperature. Potential transmittance exceeds in-situ transmittance by 0.6% at 5000db. the difference falling (approximately linearly) to zero at the surface.

A series of plots of potential transmittance (Fig.16,17) at depths in excess of 3500db reveal the general character of the transmittance in the lower part of the water volume and, by inference, of the resuspended sediment. From these plots the maximum transmittance change from the clear water maximum rarely exceeds 0.2% and sometimes approaches the sensitivity of the instrument (about .03%). These typical profiles are in striking contrast to measurement in the western north Atlantic where the bottom values for transmittance are as low as 30%[21]. Here swift bottom currents >50cm/s are found too[22].

Suspended particulate mass SPM is often correlated with the attenuance[21]. attenuance is the negative natural logarithm of the 1m transmittance. The clearest sea-water as seen by the transmissometer has been shown[23] to have an attenuance of 0.358 ±.003 or a potential transmittance PTR of 69.9 ±0.2%. The same author found a regression of SPM (in µg/kg or ppb) on attenuance C according to the expression

$$SPM = 1150(C-0.358)$$

with error typically of the order ±4µg/kg or ±20% whichever is the greater. For small changes in attenuance this expression can be conveniently be written

$$SPM = 15(69.9 - PTR)$$

The clearest potential transmittance values (Fig.16,17) appear to range from 69.4% to 68.8%: most of this variation arises we believe from material deposited on the optical surfaces of the instrument either present on launch or picked up during the passage of the instrument through the air-water interface. (The manufacturer's claim is for an accuracy of no more than 0.5%.) Any obscuring of the optics biases the measurements low so that we would tend to choose the upper values for maximum clarity. This yields minimum SPM of 8 ±4µg/kg. quite consistent with weight determinations of filtered samples[24].

The decrease in transmittance from the clear water minimum is not dependent on small obscuration of the optics and gives rise to increases of only 3 or 4 µg/kg near the sea bed. The smallness of these values can be seen by integrating the transmittance deficit up to the transmittance maximum yielding a 'standing crop' of about 1 gm m^{-2} which is somewhat lower than the 2-5gm m^{-2} reported earlier[25]. The bottom concentrations of this older study, viz 3µg/kg are however quite comparable with those reported here but the earlier reports yield much shallower depths for the clearest water and hence integration for standing crop estimates over a greater depth. The reasons for this discrepancy is, however, not known[22]. The map of standing crop for the Atlantic produced in the earlier work clearly reflected the interaction of the bottom circulation with the sediment[25] and the very low values reported here correspond to the weak currents seen at GME and other sites in the basin[1].

MOORED TRANSMISSOMETER MEASUREMENTS AT GME

A transmissometer of the type described in the previous section was also moored at GME, about 2 miles north of the PLAIN site for the period of the third deployment of the current meter moorings. The purpose of the moored transmissometer measurement was to measure fluctuations in transmittance and hence suspended particle mass near the sea-bed and to seek a relationship between these fluctuations and the strength of bottom currents.

The transmissometer and battery pack were interfaced with an IOS Mk.4 tide gauge (loaned by R. Spencer, IOS, Bidston) to record transmittance measurements every 30 minutes. The logger tube was mounted vertically between two five feet rods and above the tube the transmissometer was mounted horizontally. Rods, plates, clamps, nuts and bolts were all manufactured from Titanium. The mooring (Fig.18) consisted of a chain anchor clump, pair of IOS releases, logger/transmissometer assembly, 50m of 8mm polyester braid line and buoyancy provided by 1 x 10" diameter and 4 x 17" diameter glass spheres.

Two deployments and recoveries were made: for details see table 6.

TABLE 6

Transmissometer mooring details - GME Plain

Latitude	Longitude	Depl.	Set/recover from	Date	Duration days
33 33.6N Mooring 402	24 43.4W	1	C. Darwin 9A/85 Discovery 159	20-XI-85 21-V-86	183
31 33.6N Mooring 402X	24 43.3W	2	Discovery 159 Discovery 162	25-V-86 24-IX-86	123

On the first deployment instrument 80-117 was used; after 3 years of quite heavy use, which culminated in a leakage of sea-water via a cracked connector, its performance was not A1. On a station prior to deployment as mooring 402 it exhibited large differences in transmittance profiles between down- and up-casts. This had never happened before but we felt obliged to launch it on the mooring as we had no alternative instrument or cruise. On the deployment of mooring 402X a nearly brand-new instrument 85-035 was used: as will be seen the performance of the second instrument was somewhat different.

Plots of uncorrected transmittance versus time for both deployments are shown in the lowest panel of Fig.19. Both show a marked fall of signal with elapsed time. The change is not due to a zero drift but to a progressive reduction in sensitivity resulting from (a) decrease in output of light source with time (1% per 1000 hours of operation) and (b) obscuration of optics by unidentified brown 'mud'. Given a duty cycle of 1 in 8 the decrease observed for the second instrument is about 1.5 times that expected under (a) above. The instrument of the first deployment shows a more rapid and erratic fall which cannot be attributed to the decline in the light source. If the overall decrease in sensitivity from 68 to 66.5% results fom deposition on the optical surfaces, a smooth decrease with time is likely (the sensitivity loss depends on the integral of the rate of deposition and hence on the integral of the concentration in the water). Thus to estimate the sensitivity as a function of time a smooth (quadratic) curve has been fitted to the elevated parts of the in-situ transmission measurements. Differences between the measurements and the smooth curve have been plotted in the centre panel. For the second deployment a linear decrease sensitivity is assumed. The differences plotted are supposed the best of estimate of the transmittance, but having an uncertain origin. In the upper panel a plot of the currents 10m above the sea-bed from the PLAIN is shown.

The records from the two deployments are somewhat different in character: the first shows a decrease in transmittance over 10-30 day intervals of magnitude 0.1-0.4%, the second is much quieter with magnitude of change of no more than 0.1%. No attempt has been made to remove spikes from the record since it is not possible to distinguish between instrument noise and a large individual particle obscuration of the light path: without exception the spikes are single-sided, reducing transmittance. Lowered transmissometer measurements were made in the vicinity (1-3 miles) before (stn.9A/85-04), between (stn.11287), and at the end (stn.11361) of the record. The first station did not reach full depth but the second and third stations showed a near bottom decrease in transmittance of 0.20% and 0.15% respectively: these values correspond to resuspended particle concentrations of 3 and 2 µg/kg respectively. The variations observed in the centre panel correspond to resuspended particle concentrations of up to 8µg/kg.

Although the increases observed on the first deployment are not large, representing only twofold or at most threefold increase in near bottom suspended particle concentration, nevertheless such values have not been detected by lowered measurements anywhere in the Madeira basin. Either such values are quite rare, or occur only just above the sea-bed, or are an artifact of the instrument. Suppose these increases are taken at face value and are representative of the bottom mixed layer and let us seek a relationship with strong currents. There is none: correlation between (de-trended) transmittance and current speed for the entire record does not differ significantly from zero. Furthermore an examination of the period of strongest currents, in the last 15 days of 1985 and the first 15 days of 1986 again reveals no correlation with transmittance. If resuspension occurs locally it will occur at times of strongest currents and hence a correlation is expected; its absence may be taken to indicate that local resuspension does not occur.

If the resuspension occurs at some distance then the correlation of low transmittance or excess SPM with strong currents is likely to be very weak. Plumes of resuspended sediments which are carried around in the eddying currents[2] will arrive on site as the currents decay but at any site and on any occasion the extent of decay will be a random variable.

THE DISTRIBUTION OF 'HIGH SPEED' CURRENTS

It is worth emphasising that the only observations of current speeds available from GME site are the values averaged over 1 hour: short term averages will inevitably be larger. Examination of the data reveals that 10cm/s may be taken as representative of a 'high' speed at the GME site. The number of hours of data for which the 1hr-mean speed exceeds 10cm/s is shown in table 7: the numbers are scaled to 23000 hrs of observation (approximately 960 days of record) so that 23 hrs represents a frequency of 0.1%.

The site on the plain is clearly different from the other two which are dominated by the presence of the hill. On the plain the number of occasions of high speed currents is approximately independent of height whereas near and over the hill the number declines sharply with height.

TABLE 7

Some statistics of high speed currents at GME

		Plain	Hill-foot	Hill-top
No. of hrs in which speed exceeds 10cm/s	10m.a.b.	71	335*	284
*Normalised to 23000 hrs.	1000m.a.b.	95	40*	26
Max speed) 1st deployment		12.2cm/s	15.3	15.2
10m.a.b.,) 2nd deployment		11.6	12.1	12.7
cm/s) 3rd deployment		11.3	-	11.1
Fifty year return value 10m.a.b, cm/s		14 ±1	18 ±1	18 ±1

At a height 10m above the sea-bed the frequency of speeds exceeding 10cm/s is only one quarter on the plain of that on the hill-top and at the hill-foot. The maximum observed speed at these latter sites is 15cm/s compared with 12cm/s on the plain.

The probability that a data period (1 hr) has a speed less than a certain value has been derived from the observations and plotted against speed using Weibull, Fisher-Tippett I and lognormal distributions[26]. The plots using a Weibull distribution yield an approximately linear relationship at the three sites, Figs.20-22, allowing extrapolation to be made. The right hand margin of Figs.20-22 represents a complementary probability of 2×10^{-6}, viz. 1 hr in

5×10^5 hrs or approximately 50 years. Thus by extrapolation to this margin, the mean speed exceeded on average for only ONE hour in fifty years is found. The values are shown in the bottom row of table 7 and the errors are estimates of the uncertainty of extrapolation only. As expected the hill dominated values exceed that on the plain but all are less than 20 cm/s.

EROSION OF SEDIMENT BY CURRENTS

Are these currents sufficient to erode the sediments? According to P. Schultheiss (private communication) the median particle diameter for the surface sediments on the plain at GME is 3-4μ: the grains have a density of 2.6g cm^{-3} and are only 'weakly' cohesive. Ignoring the cohesion, the fineness of the sediment and the weakness of the current suggests strongly that the surface will be hydrodynamically smooth (which is verified a posteriori). A review[27] of the measurements and theory describing the conditions in which the sediment grains begin to move suggest the expression

$$\frac{\rho u_*^2}{(\rho_d - \rho) g D} \approx 0.1 \left(\frac{u_* D}{\upsilon}\right)^{-0.3}$$

where u_* is (here) the critical friction velocity for initial motion

ρ is the density of sea water, υ its kinematic viscosity

g the acceleration of gravity

D is the median particle diameter and ρ_d its density.

Employing the values given above and $g = 10^3$ $cm^2 s^{-1}$ $\upsilon = 1.6 \times 10^{-2} cm^2 s^{-2}$ yields

$$u_*(crit) \approx 0.5 cms^{-1}$$

Note that as u_* progressively exceeds $u_*(crit)$ so the erosion of the sediment grows and the resuspended particle concentration increases.

The friction velocity on the surface and the mean flow at some height are related through the drag coefficient thus:-

$$u = u_*/\sqrt{C_D}$$

The only measurements made in the deep ocean under weak flow conditions over a smooth bottom similar to GME[28] gave

$$C_D = 1.9 \times 10^{-3}$$

where the mean flow was measured 0.5m above the sea bed. The latter is less

than that measured at a height of 10m by a factor of $^2/3^2$, so that the mean flow measured at 10m required to set the sediment in motion is

$$u \approx u_*(\text{crit}) \times 34 \approx 17 \text{ cm/s}$$

This value does depend on the drag coefficient, it should be noted, and decreases as the drag coefficient increases. It also takes no account of any cohesive forces between the grains of the sediment and therefore is a conservative estimate.

The threshold value for particle movement is thus approximately equal to the value of the 50 year return value around the hill and somewhat higher than that on the plain. Certainly without further information about the cohesiveness of the sediments we cannot exclude the possibility of very infrequent erosion of the sea-bed from GME, the suspension of material into the benthic boundary layer and its transport over considerable distances.

The existence of a non-zero standing crop of resuspended particles in the NE Atlantic (vide earlier section) requires, of course the existence of some agency of resuspension. Apart from bioturbation, current erosion appears the major contender. In table 8 the occurrence of near bottom speeds considerably in excess of those measured at GME (table 7) are documented. These examples occur at somewhat shallower depths than the abyssal plain and therefore on its margin. The maximum speed observed and known to the author of 30cm/s observed 10m above the bottom is confirmed by a measurement of 27cm/s some 90m shallower and probably exceeded the local threshold for sediment movement. A plume of sediment could then be swept off the rise and settle slowly through the deeper and clearer waters. Fig.15 (near 4000db) illustrates this phenomenon.

About 200km to the north of GME, and on the abyssal plain, strong near bottom current events have been shown to be related to a strong near-surface current jet[29]. So far the measured bottom currents there do not exceed those at GME. Thus the approach to GME of the near-surface jet, because of a climatological fluctuation, would not appreciably change the climatology of the strong near-bottom currents presented in this report.

TABLE 8

High Speed Near-bottom Currents on and around the Madeira Abyssal Plain

Source/ Identification	Lat, N	Lon, W	Depth, m	Duration, days	Max hourly speed, cm/s
IFM Kiel 277207	34 48	23 05	4722	220	19.8
MAFF 81-18	32 00	20 00	4461	255	22.5
IOS[2] 34402	32 16	20 13	4669	120	30.3

ACKNOWLEDGEMENTS

The author wishes to thank Messrs Goy, Gwilliam, Moorey, Phillips, Smithers and Waddington for their assistance with CTD and transmittance measurements and moored current meter observations; also the officers and crew of both the RVS Charles Darwin and RRS Discovery for their wholehearted assistance at sea. The contributions of Drs R.T. Pollard, W.J. Gould and J.C. Swallow, both at sea and ashore, are also gratefully acknowledged.

TABLE 9

Mean Currents and Temperatures, by Deployment

Site	a.b. m	Deploy #	East cm/s	North cm/s	σ_E cm/s	σ_N cm/s	temp. °C	σ_T °C	θ °C
PLAIN	1000	1	-0.67	-0.02	2.32	2.56	2.444	.0056	2.048
		2	-1.18	-0.11	2.55	2.57	2.452	.0094	2.056
		3	-0.99	-0.57	2.34	2.98	2.464	.0069	2.065
	100	1	-0.87	-0.06	2.94	3.26	2.482	.0020	1.956
		2	-0.35	0.03	2.64	2.62	*	*	*
		3	-0.89	-0.42	2.77	3.16	2.488	.0022	1.961
	10	1	-0.84	0.28	3.08	3.11	2.492	.0004	1.953
		2	-0.61	0.23	3.11	2.74	2.492	.0008	1.953
		3	-0.90	-0.65	2.31	3.12	2.496	.0025	1.956
HILL-FOOT	1000	1	*	*	*	*	*	*	*
		2	-0.04	-0.81	3.02	3.05	2.435	.0074	2.039
		3	*	*	*	*	*	*	*
	100	1	-0.68	-1.99	3.31	3.27	*	*	*
		2	-0.19	-1.95	2.70	3.06	2.473	.0022	1.949
		3	*	*	*	*	*	*	*
	10	1	-0.43	-2.06	3.16	3.10	2.494	.0017	1.961
		2S	-1.05	-2.05	2.32	2.68	*	*	*
		3	*	*	*	*	*	*	*
HILL-TOP	1000	1	-0.19	-0.23	2.83	2.30	2.482	.0076	2.138
		2	-0.15	0.22	3.35	2.93	2.486	.0100	2.142
		3	*	*	*	*	*	*	*
	100	1	1.19	0.51	3.00	2.83	*	*	*
		2	1.30	-0.03	3.24	2.99	2.423	.0041	1.959
		3	1.19	-1.27	3.13	2.88	2.439	.0055	1.965
	10	1	1.41	0.13	3.59	2.57	2.439	.0028	1.960
		2	1.32	0.22	3.48	2.87	2.431	.0047	1.954
		3	1.28	-0.92	3.32	2.90	2.446	.0031	1.960
GME BOX	3	1	-1.20	1.46	3.01	3.29	2.494	.0046	1.953

S denotes shortness of record: consult table 2 for duration of each record

TABLE 10

Mean Speeds and Percent Stall, by deployment

Site	ht. above bottom, m.	mean speed, cm/s 1	2	3	percent stall 1	2	3
PLAIN	1000	2.90	3.24	3.32	52	44	61
	100	4.03	3.24	3.86	14	42	32
	10	3.97	3.69	3.58	16	31	38
HILL-FOOT	1000	3.87	3.91	*	22	18	*
	100	4.56	3.96	*	12	21	*
	10	4.22	3.52S	*	19	36S	*
HILL-TOP	1000	3.16	3.98	*	35	23	*
	100	3.75	4.09	4.25	24	26	15
	10	4.04	4.13	4.28	19	24	19
GMEBOX	3	*	4.30	*	*	18	*

S denotes shortness of record: consult table 2 for duration of each record

REFERENCES

1. Dickson, R.R., W.J. Gould, T.J. Muller and C. Maillard, 1985: Estimates of the mean circulation in the deep (>2000m) layer of the eastern North Atlantic. In 'Essays on Oceanography - a tribute to John Swallow'. Progress in Oceanography, Vol.14, Pergamon Press, Oxford, 103-128.
2. Saunders, P.M. and K.J. Richards, 1985: Benthic boundary layer, IOS observational and modelling programme, Final report. IOS Report No.199, 61pp.
3. Searle, R.C., P.J. Schultheiss, P.P.E. Weaver, M. Noel, R.B. Kidd, C.L. Jacobs and Q.J. Huggett, 1985: Great Meteor East (Distal Madeira Abyssal Plain): Geological studies of its suitability for disposal of heat-emitting radioactive wastes. IOS Report No.193, 161pp.
4. Saunders, P.M. and J.W. Cherriman, 1983: Abyssal temperature measurements with Aanderaa current meters. Deep-Sea Res., 30, 663-667.
5. Saunders, P.M., 1986: Moored current meter data from the Madeira abyssal plain (GME) 1st deployment 1984. IOS Report No.221, 47pp.
6. Saunders, P.M., 1986: Ibid, 2nd deployment 1985. IOS Report No.228, 50pp.
7. Flierl, G.R. and J.C. McWilliams, 1977: On the sampling requirements for measuring moments of eddy variability. J. Mar. Res., 35, 797-820.
8. Taylor, G.I., 1921: Diffusion by continuous movements. Proc. London Math. Soc., A20, 196-211.
9. Gould, W.J., R. Hendry and H.E. Huppert, 1981: An abyssal topographic experiment. Deep-Sea Res., 28, 409-440.
10. Owens, W.B. and N.G. Hogg, 1980: Oceanic observations of stratified Taylor columns near a bump. Deep-Sea Res., 27, 1029-1045.
11. Huppert, H.E., 1975: Some remarks on the initiation of inertial Taylor columns. J. Fluid Mech., 67, 397-412.
12. Saunders, P.M., 1987: Flow through Discovery Gap. J. Phys. Oceanogr. (In press.)
13. Saunders, P.M. and F. Dolan, 1987: CTD data from Discovery Gap and the Madeira abyssal plain. IOS Report No.236, 76pp.
14. Coats, D.A., 1981: An estimate of absolute geostrophic velocity from the density field in the northeastern Pacific ocean. J. Geophys. Res., 86, 8031-8036.
15. Olbers, D.J., M. Wenzel and J. Willebrand, 1985: The inference of North Atlantic circulation patterns from climatological hydrographic data. Reviews of Geophys., 23, 313-356.

16. Schwiderski, E.W., 1979: Global ocean tides, part II: the semidiurnal principal lunar tide (M_2), Atlas of tidal charts and maps. NSWC TR 79-414, Naval Surface Weapons Center, Virginia.

17. Priestley, M.B., 1981: In Chapter 9.5 of Spectral analysis and time series - Vol.2: Multivariate series, prediction and control. Academic Press, London, 890pp.

18. McWilliams, J.C. and A.R. Robinson, 1974: A wave analysis of the Polygon array in the tropical Atlantic. Deep-Sea Res., 21, 359-368.

19. Bartz, R., J.R.V. Zanevald and H. Pak, 1978: A transmissometer for profiling and moored observations in water. Soc. Photo. Opt. Instrum. Eng., 160, 102-108.

20. Saunders, P.M. and A. Manning, 198?: CTD data from the northeast Atlantic Ocean, 22°N - 33°N, 19°W - 24°W July 1983 during RRS Discovery Cruises 138, 139. IOS Report No.188, 114pp.

21. Gardner, W.D., P.E. Biscaye, J.R.V. Zaneveld and M.J. Richardson, 1985: Calibration and comparison of the LDGO and the OSU transmissometer on the Nova Scotian rise. Marine Geol., 66, 323-344.

22. Richardson, M.J., M. Wimbush and L. Mayer, 1981: Exceptionally strong near-bottom flows on the continental rise of Nova Scotia. Science, 213, 887-888.

23. Bishop, J.K.B., 1986: The correction and suspended particulate matter calibration of Sea Tech transmissometer data. Deep-Sea Res., 33, 121-134.

24. Brewer, P.G., D.W. Spencer, P.E. Biscaye, A. Hanley, P.L. Sachs, C.L. Smith, S. Kadar and J. Fredericks, 1976: The distribution of particulate mattter in the Atlantic Ocean. Earth and Planetary Sci. Lett., 32, 393-402.

25. Biscaye, P.E., and S.L. Eittreim, 1977: Suspended particle loads and transports in the Nepheloid layer of the abyssal Atlantic Ocean. Marine Geol., 23, 155-172.

26. Johnson, N.L., and S. Kotz, 1970: Continuous univariate distributions - 1. Houghton, Mifflin Co., Boston, 300pp.

27. Sleath, J.F.A., 1984: In Chapter 6 Section 7 of Sea Bed Mechanics. Jonn Wiley and Sons, New York, 335pp.

28. Elliott, A.J., 1984: Measurements of turbulence in an abyssal boundary layer. J. Phys. Oceanogr., 14, 1780-1786.

29. Siedler, G., Zenk, W., and W.J. Emery, 1985: Strong-current events related to a subtropical front in the Northeast Atlantic. J. Phys. Oceanogr., 15, 885-897.

FIGURE CAPTIONS

Figure 1 Map of GME study site showing mooring locations: in parenthesis number of successful recoveries.

Figure 2 Schematic cross-section of the 3 moorings and 9 current meters utilised in this report.

Figure 3 Record mean currents; solid 10m, dashed 1000m above sea-bed.

Figure 4 Virtual displacement of water 10m above plain: 25 day intervals are indicated as +.

Figure 5 Virtual displacement of water 10m above bottom at hill-foot: 25 day intervals are indicated as +.

Figure 6 Virtual displacement of water 10m above hill-top: 25 day intervals are indicated as +.

Figure 7 Inviscid flow of uniform rotating fluid over a cone-shaped obstacle[11]. The flow parallels the streamlines and its speed varies inversely with their spacing.

Figure 8 E-W section of potential temperature versus pressure (depth) on 31°30'N: note the doming of the isotherms over the hill.

Figure 9 25 day mean current vectors from selected steady flow periods: speeds in cm/s.

Figure 10 Current profile derived from hydrographic data for region 30-35°N, 21-26°W. The origin is determined as indicated in the text; upper[15], lower[14].

Figure 11 Variance spectrum of east component of current 10m and 1000m above bottom: solid-plain, dashed-hill top.

Figure 12 Variance spectrum of north component of current 10m and 1000m above bottom: solid-plain, dashed-hill top.

FIGURE CAPTIONS (continued)

Figure 13 Time series of current components on plain: origin is 1 Jan 1984. Solid 10m a.b.; dashed 1000m a.b.

Figure 14 Current ellipses for fluctuation with periods (1) 127-500 days. (2) 71-127 days and (3) 49-71 days; measurements 10m above plain.

Figure 15 Profile of potential transmittance versus pressure (depth) for station 10839: 32 21N, 20 13W. Note the decrease in the lowest 500db.

Figure 16 Near bottom profiles of potential transmittance (also temperature) versus pressure: sites distant from GME.

Figure 17 Near bottom profiles of potential transmittance (also temperature) versus pressure: GME study site.

Figure 18 Schematic of transmissometer mooring.

Figure 19 Measurements of currents (10m) and light transmission (3m) on the plain. Lower panel - raw data; centre panel - differences from assumed smooth drift in instrument sensitivity.

Figure 20 Probability of current speed 10m above sea-bed less than a specified value. The plot linearises a Weibull distribution: PLAIN.

Figure 21 Probability of current speed 10m above sea-bed less than a specified value. The plot linearises a Weibull distribution: HILL-FOOT.

Figure 22 Probability of current speed 10m above sea-bed less than a specified value. The plot linearises a Weibull distribution: HILL-TOP.

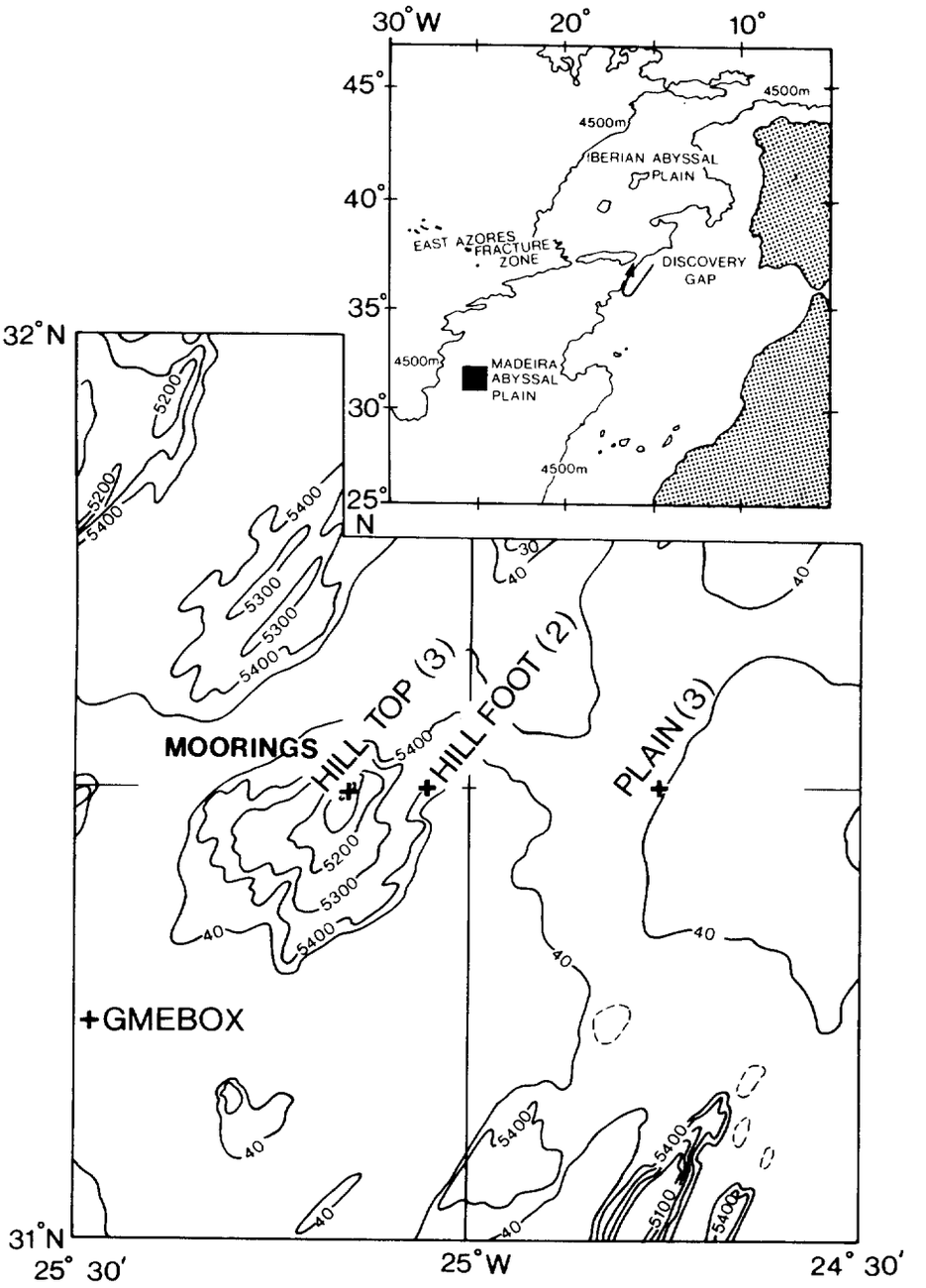

Figure 1 Map of GME study site showing mooring locations: in parenthesis number of successful recoveries.

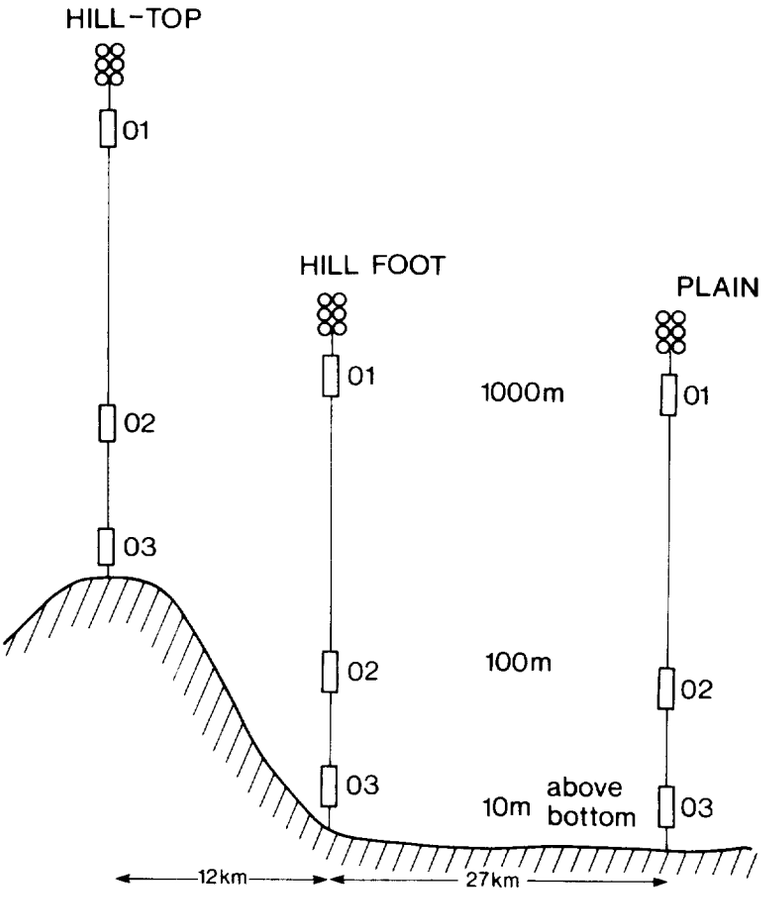

Figure 2 Schematic cross-section of the 3 moorings and 9 current meters utilised in this report.

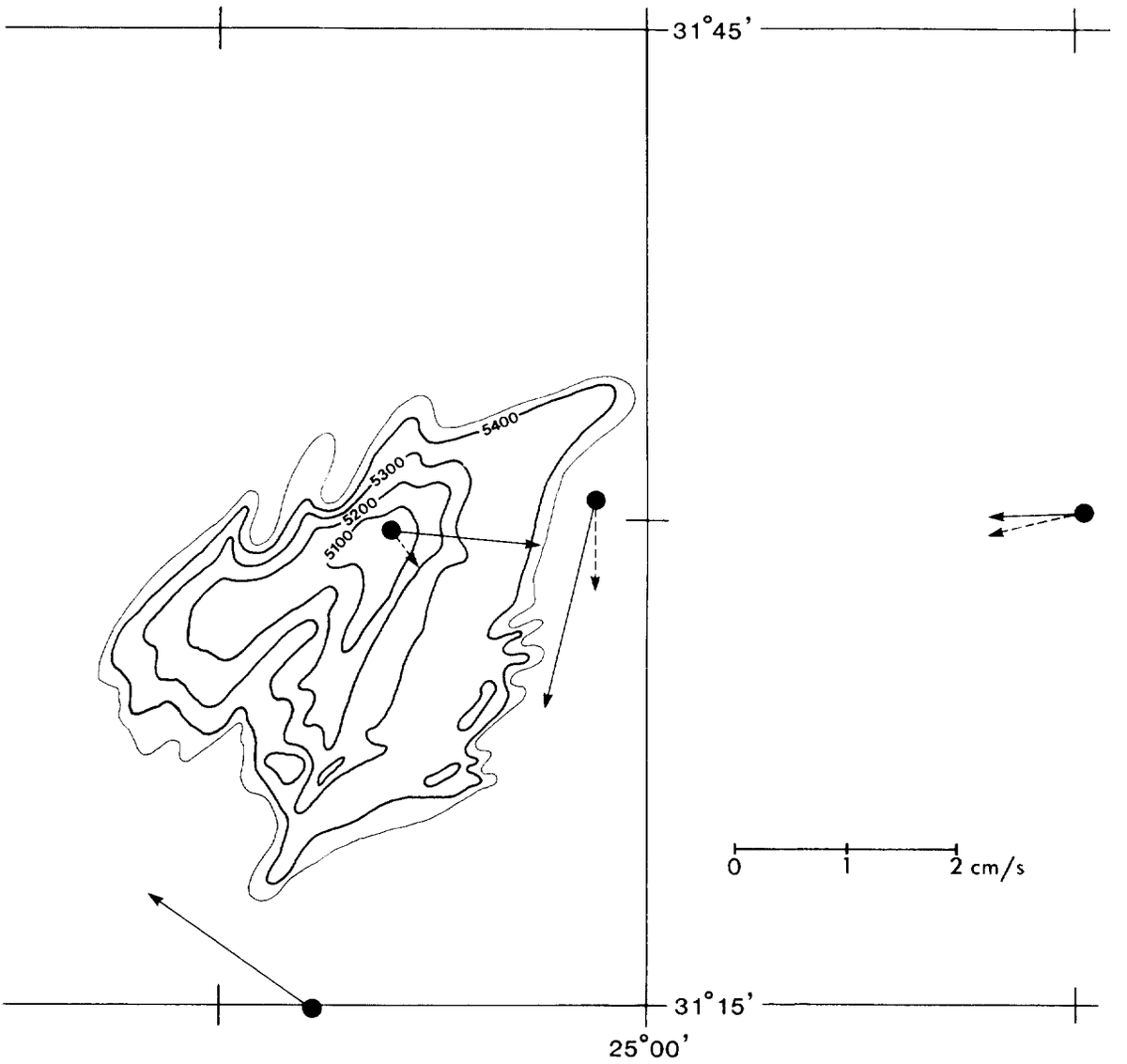

Figure 3 Record mean currents; solid 10m, dashed 1000m above sea-bed.

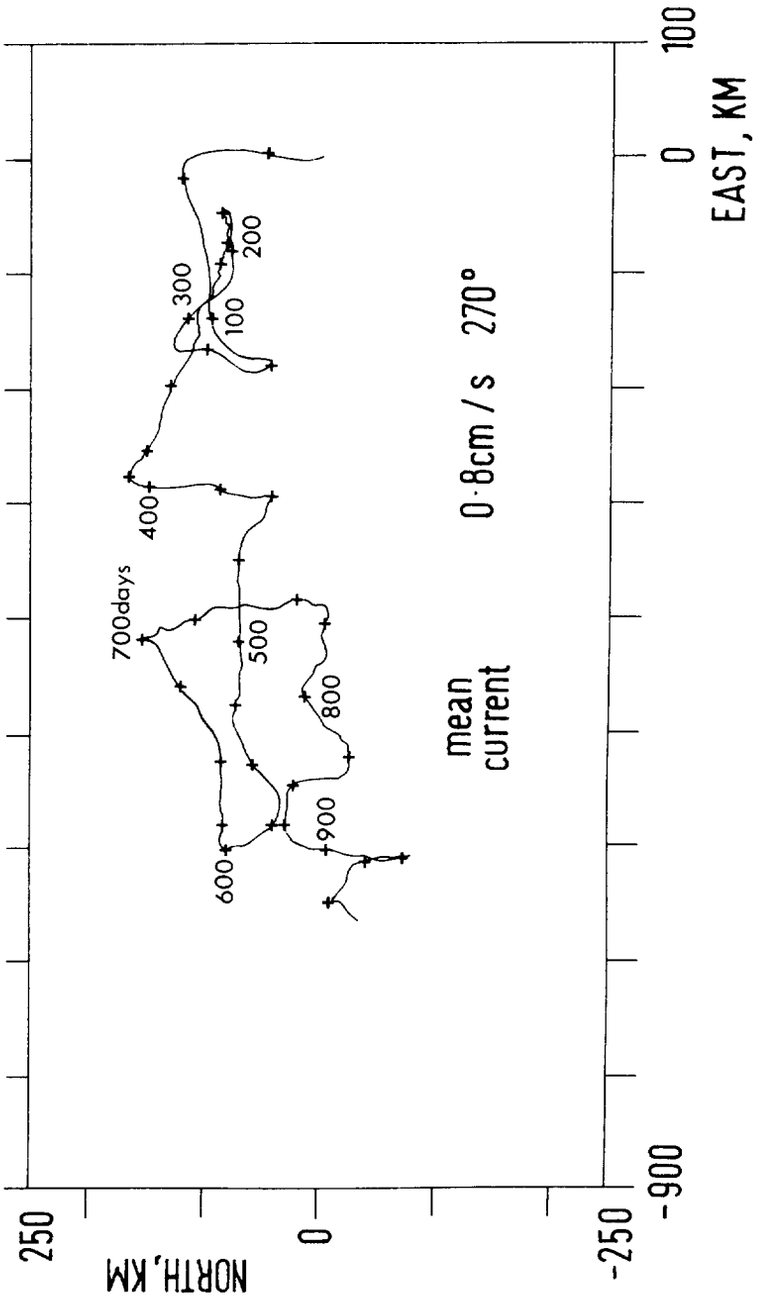

Figure 4 Virtual displacement of water 10m above plain: 25 day intervals are indicated as +.

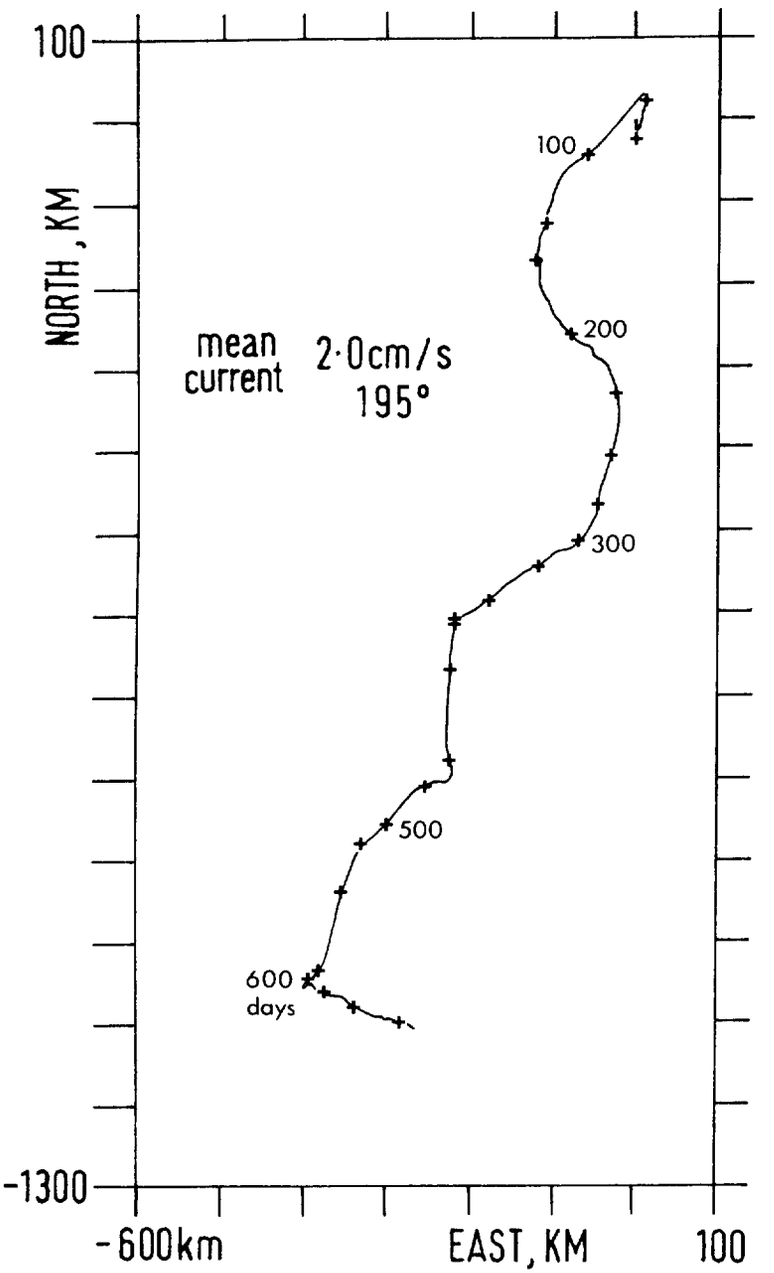

Figure 5 Virtual displacement of water 10m above bottom at hill-foot: 25 day intervals are indicated as +.

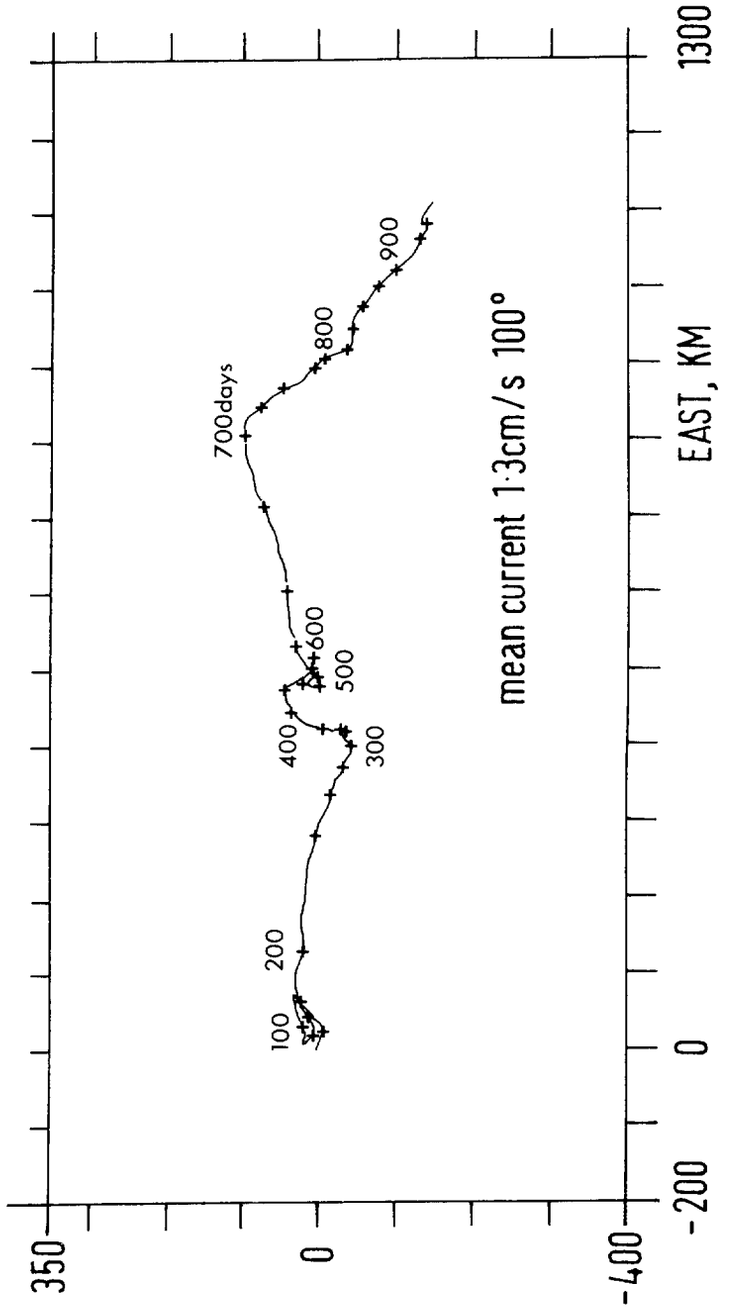

Figure 6 Virtual displacement of water 10m above hill-top: 25 day intervals are indicated as +.

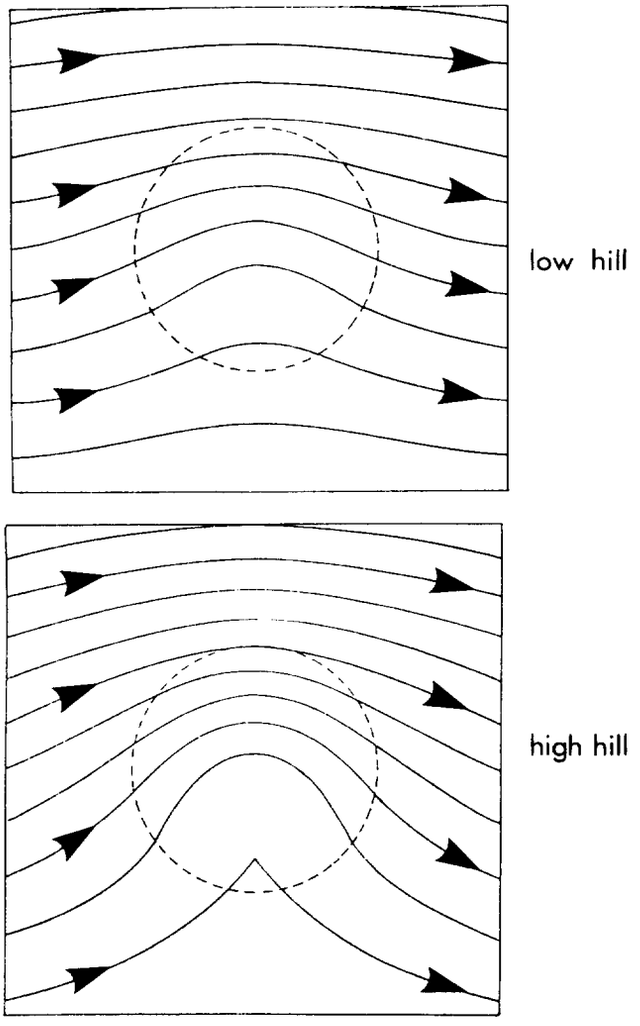

Figure 7 Inviscid flow of uniform rotating fluid over a cone-shaped obstacle[11]. The flow parallels the streamlines and its speed varies inversely with their spacing.

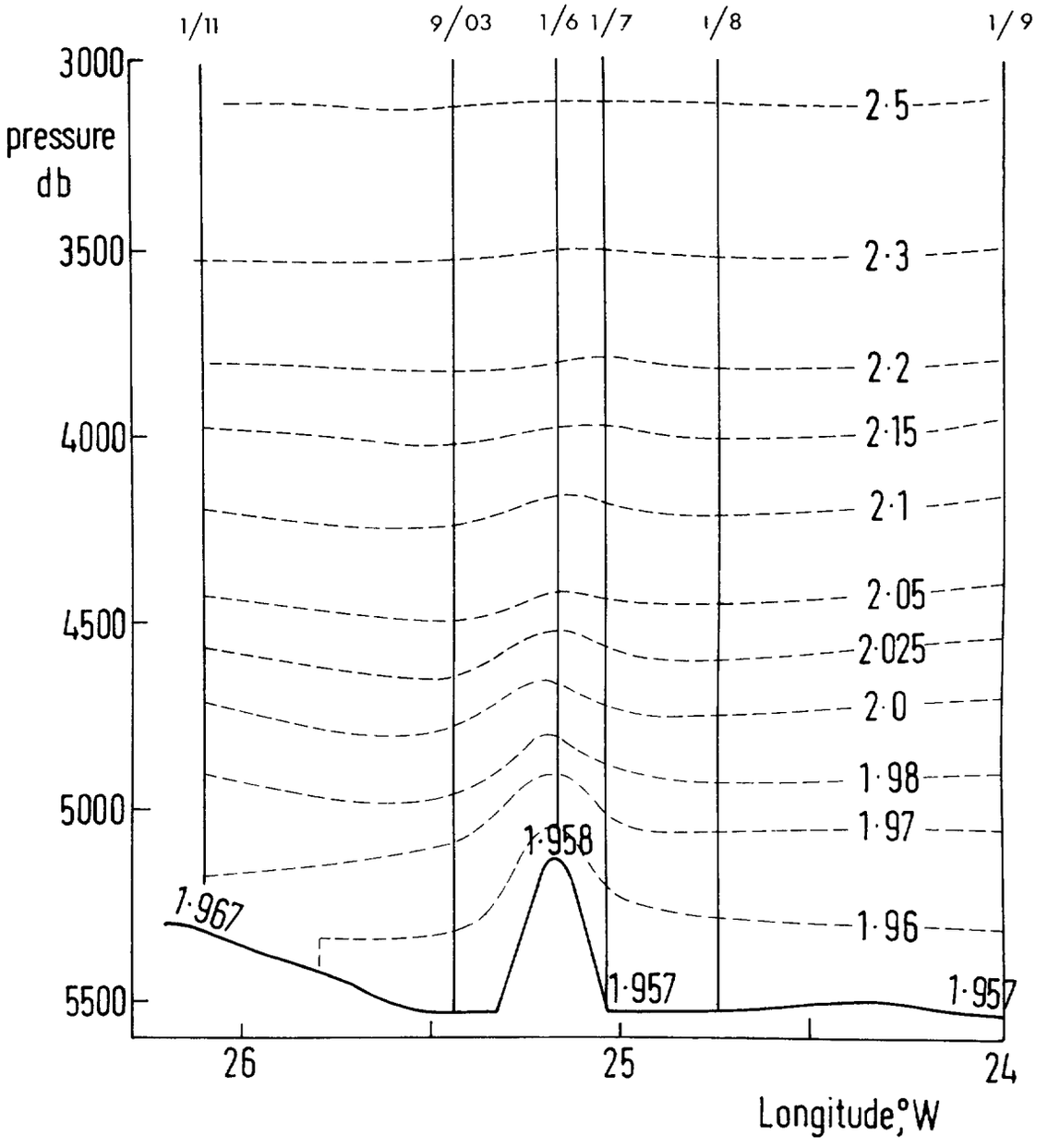

Figure 8 E-W section of potential temperature versus pressure (depth) on 31°30'N: note the doming of the isotherms over the hill.

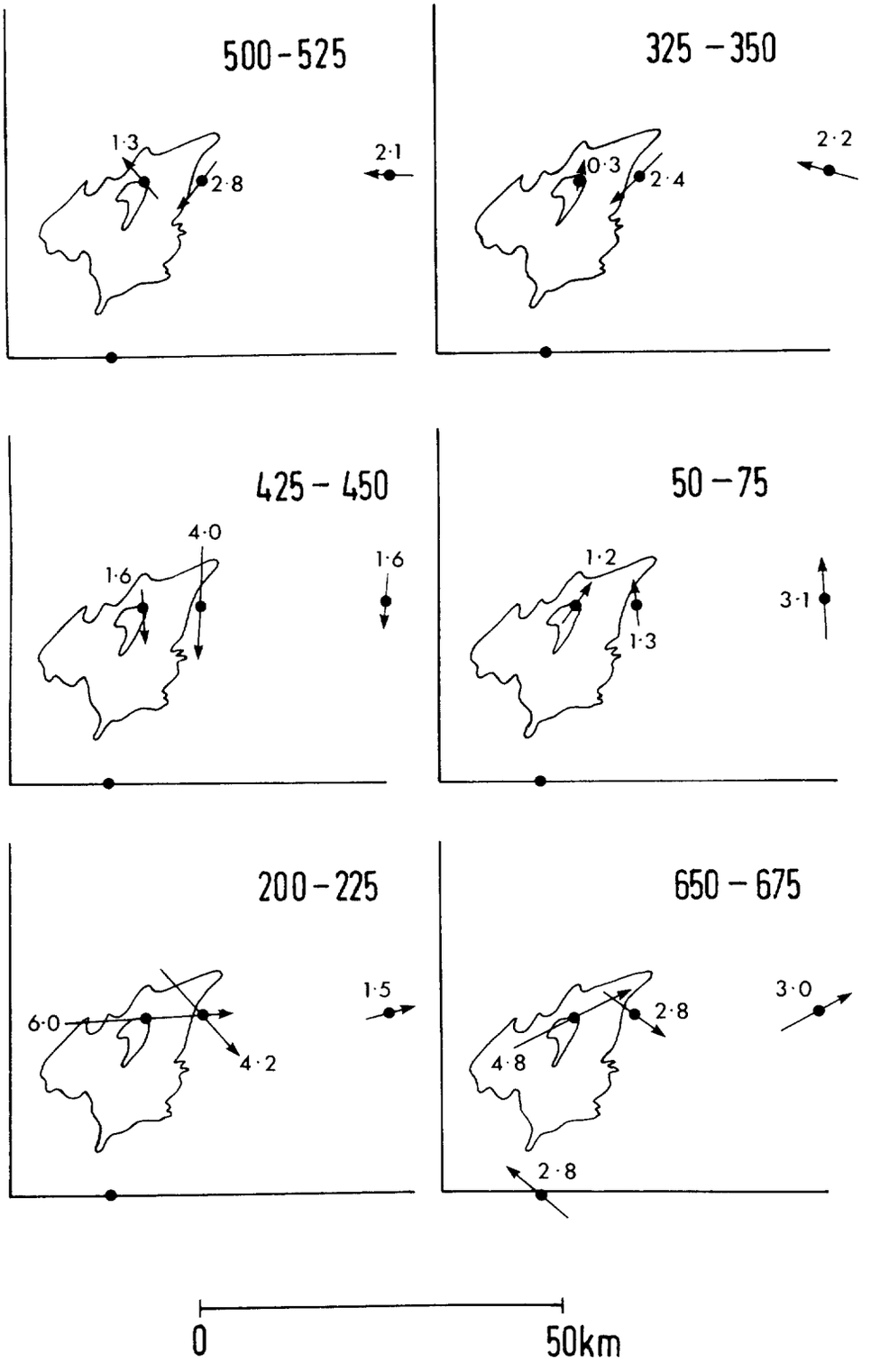

Figure 9 25 day mean current vectors from selected steady flow periods: speeds in cm/s.

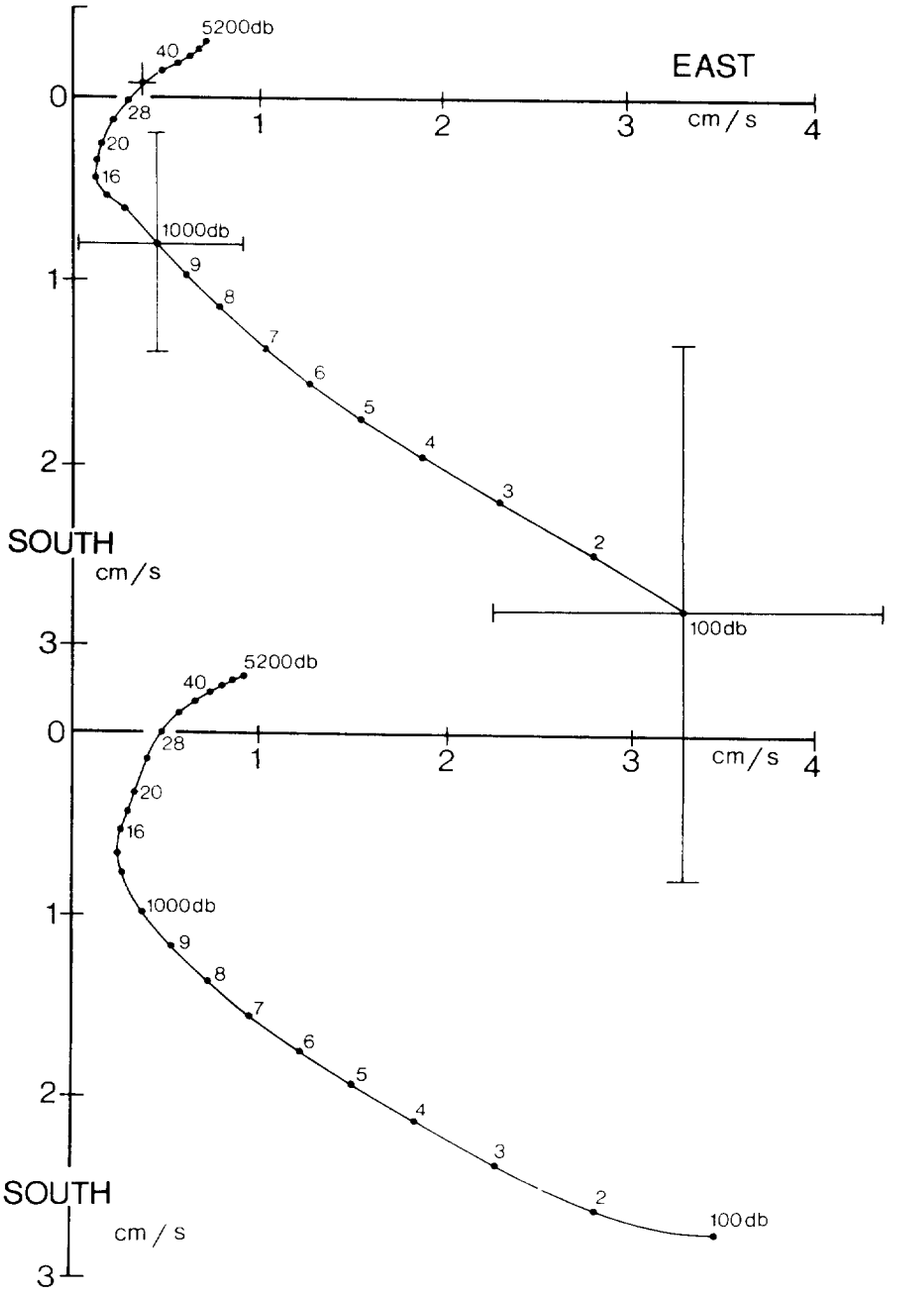

Figure 10 Current profile derived from hydrographic data for region 30-35°N, 21-26°W. The origin is determined as indicated in the text; upper[15], lower[14].

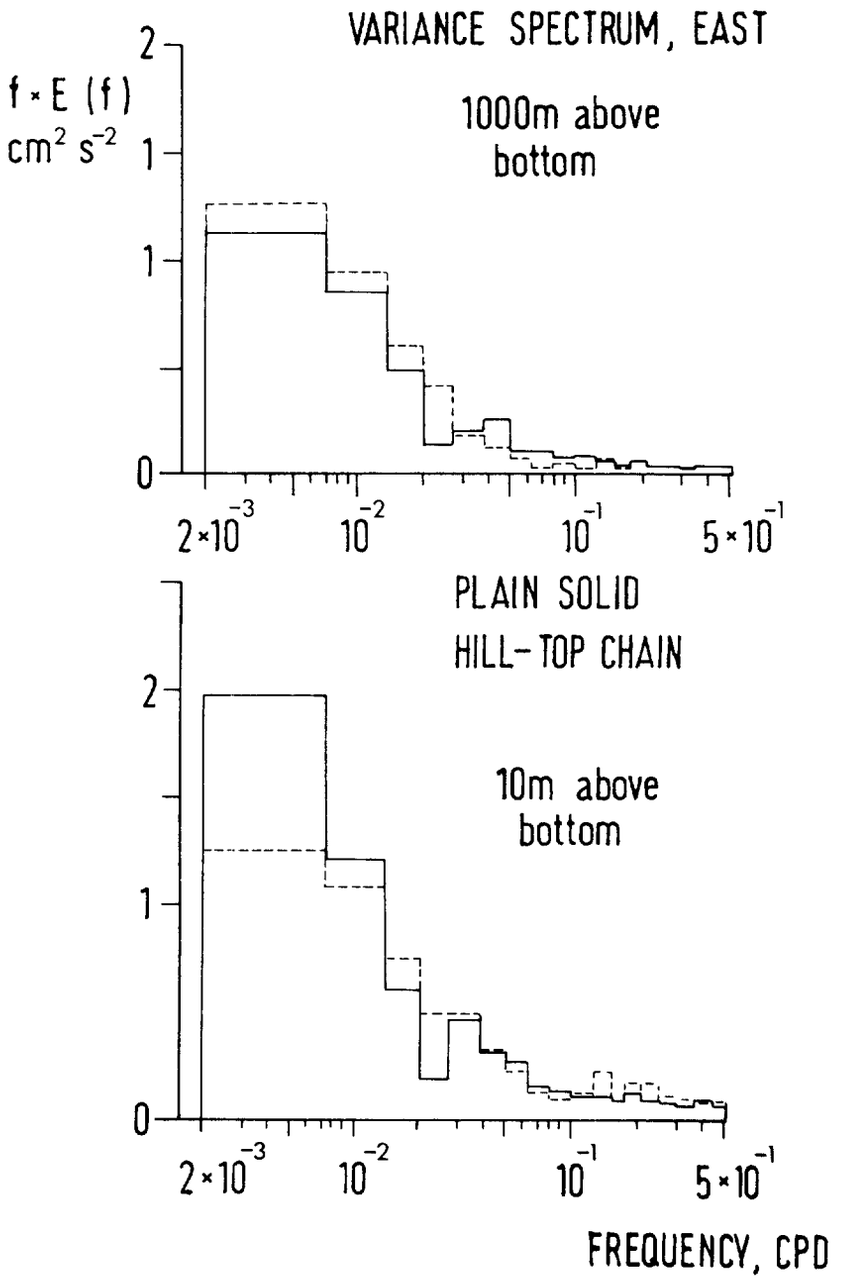

Figure 11 Variance spectrum of east component of current 10m and 1000m above bottom: solid-plain, dashed-hill top.

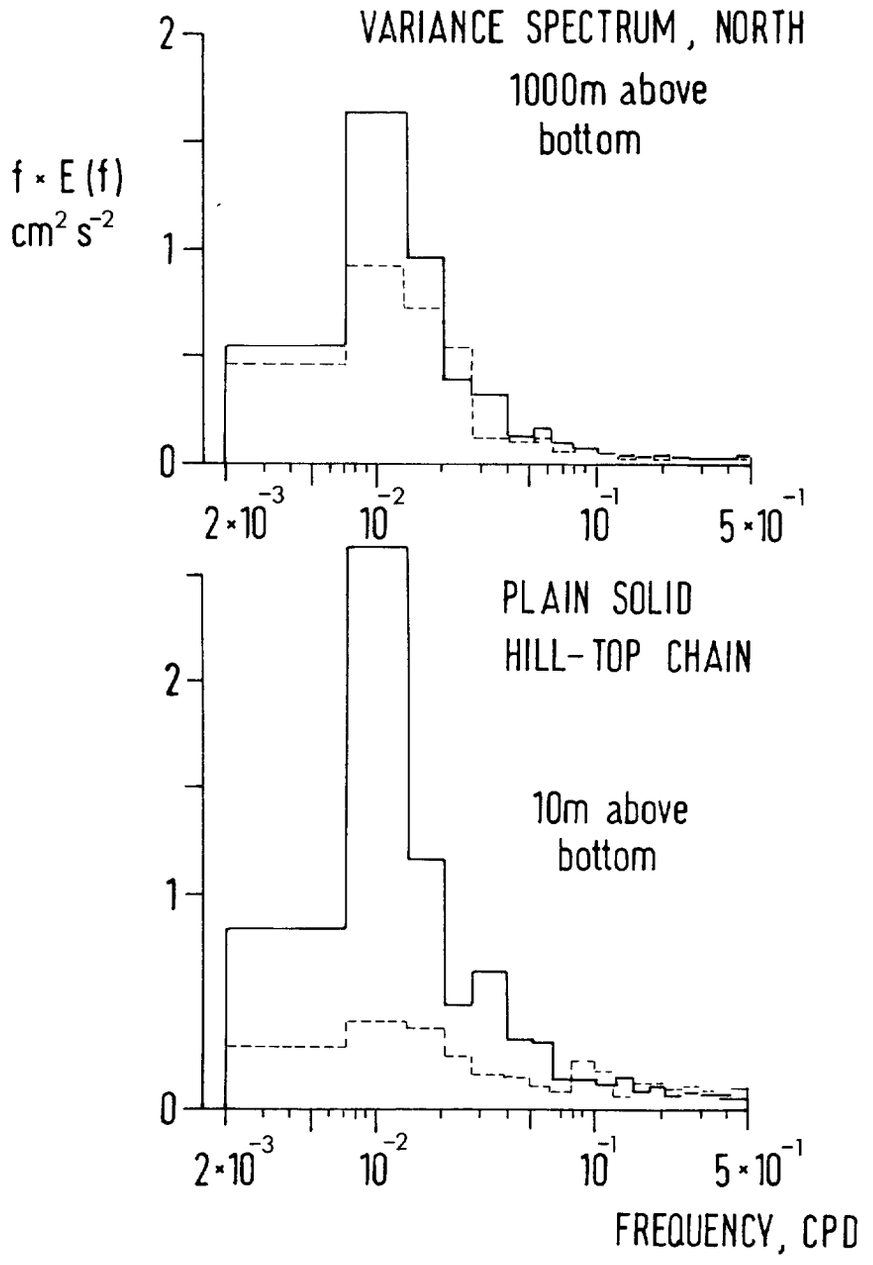

Figure 12 Variance spectrum of north component of current 10m and 1000m above bottom: solid-plain, dashed-hill top.

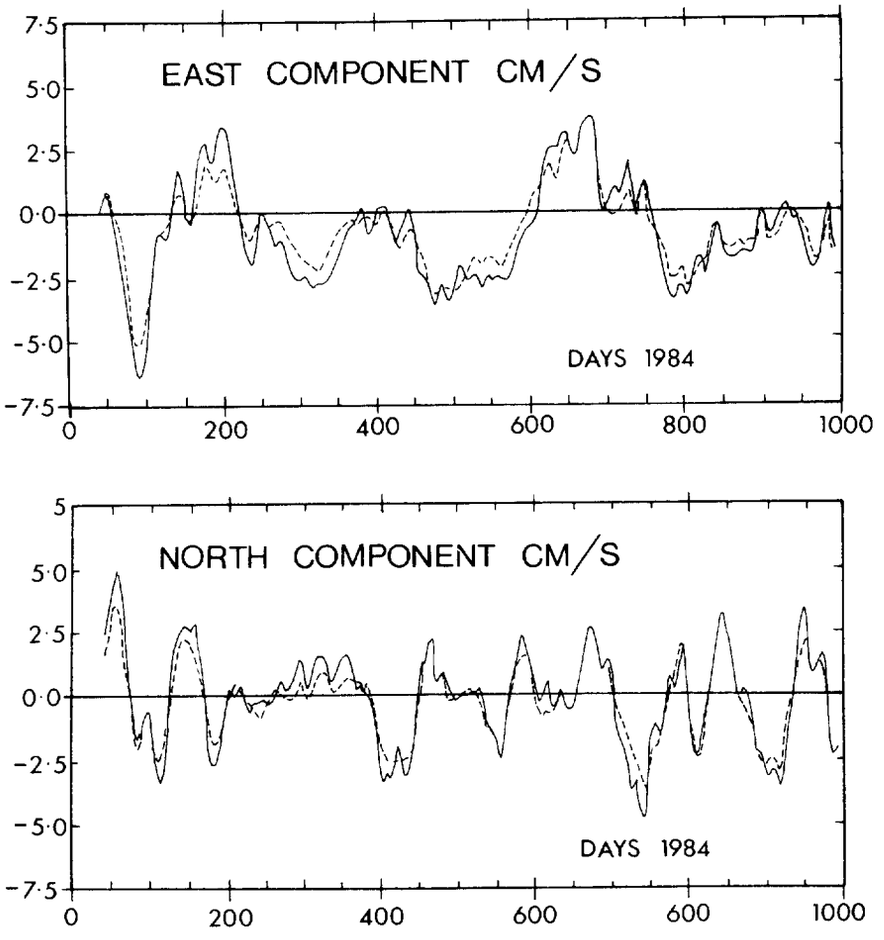

Figure 13 Time series of current components on plain: origin is 1 Jan 1984. Solid 10m a.b.; dashed 1000m a.b.

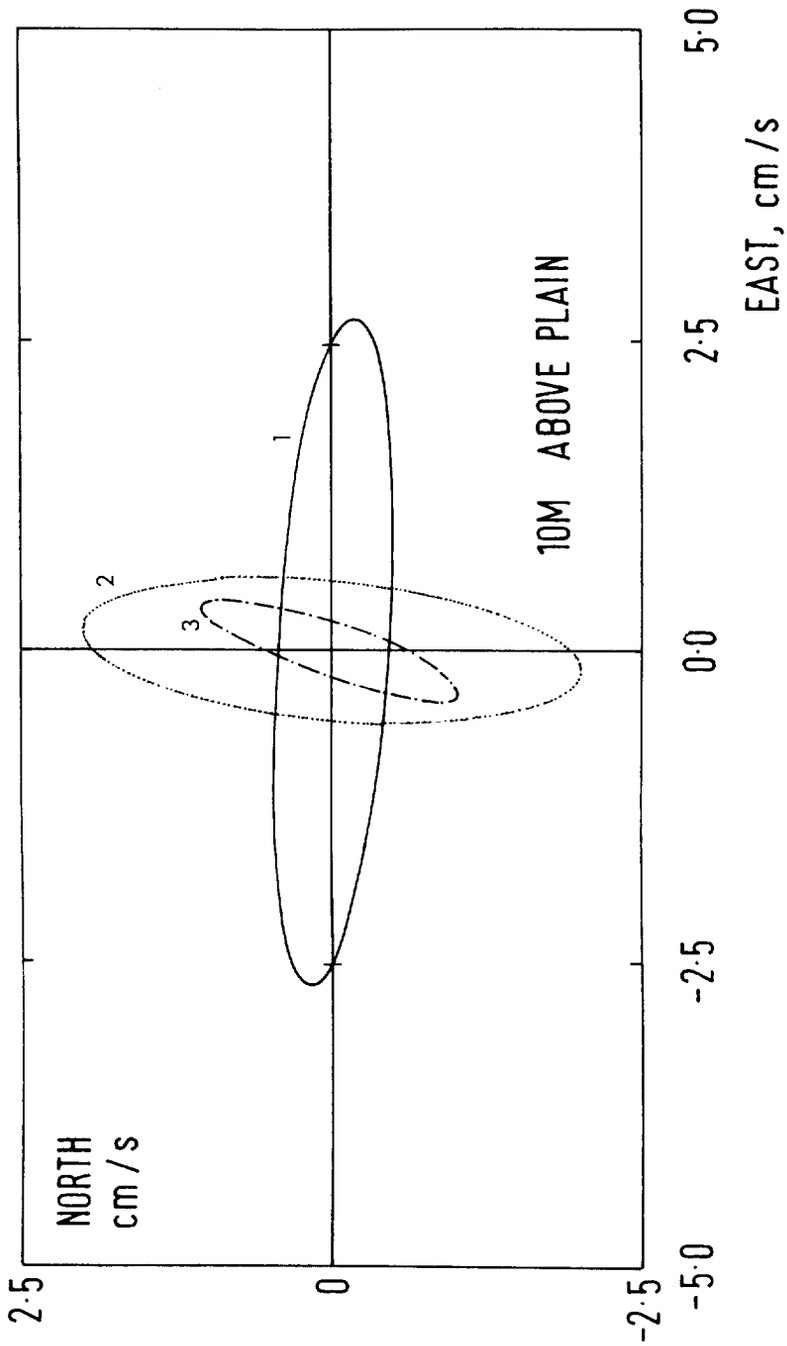

Figure 14 Current ellipses for fluctuation with periods (1) 127-500 days
(2) 71-127 days and (3) 49-71 days; measurements 10m above plain.

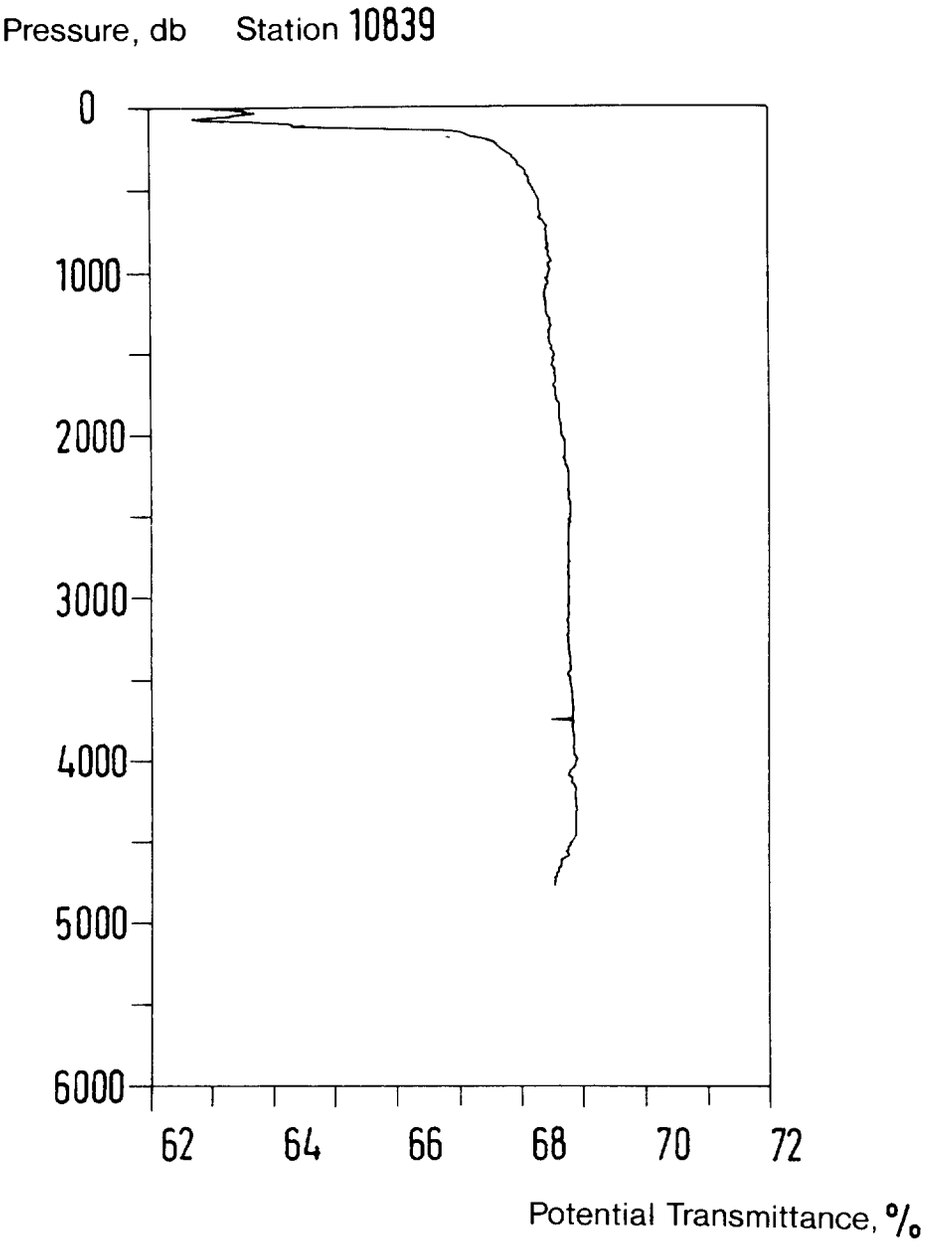

Figure 15 Profile of potential transmittance versus pressure (depth) for station 10839; 32 21N, 20 13W. Note the decrease in the lowest 500db.

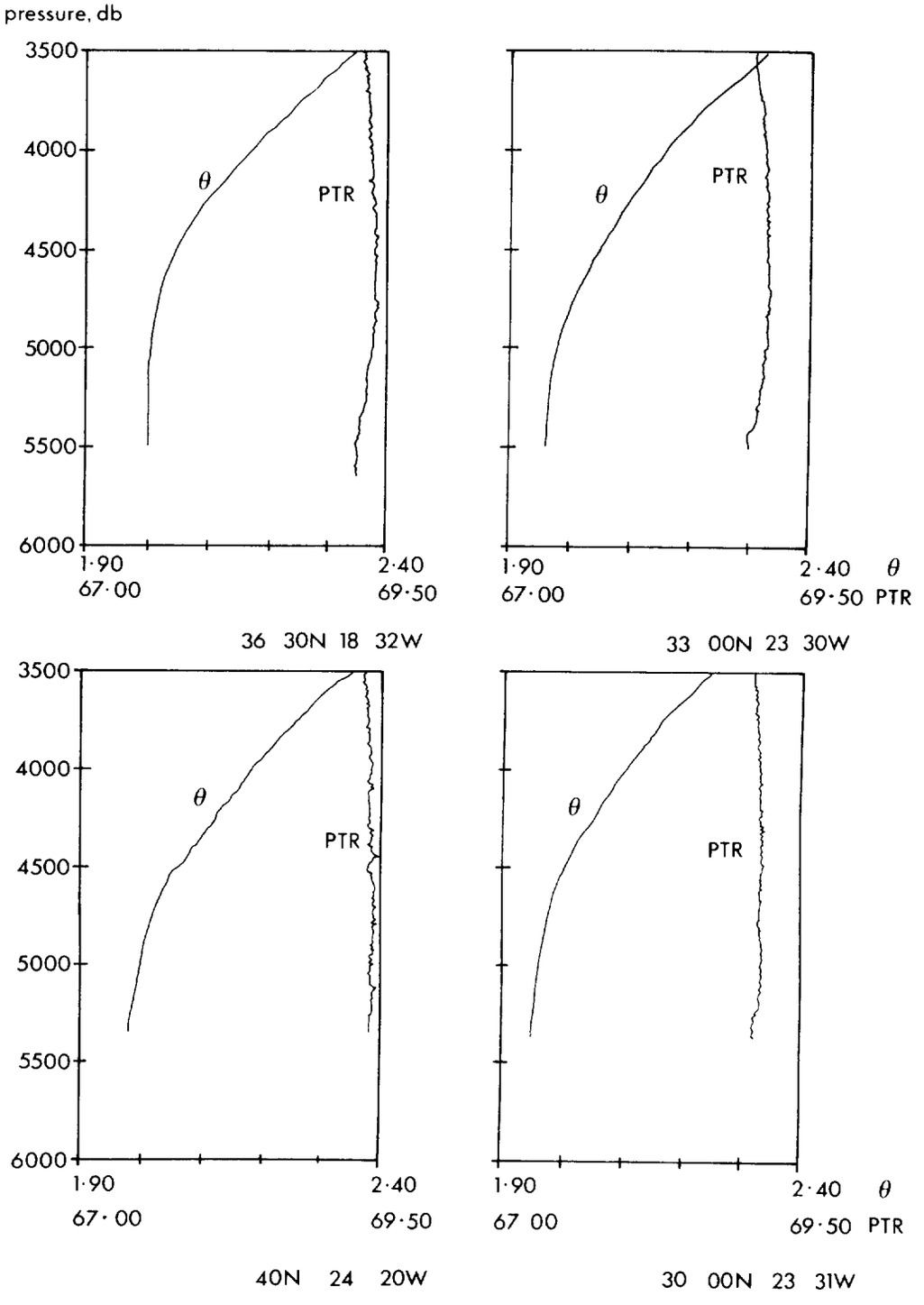

Figure 16 Near bottom profiles of potential transmittance (also temperature) versus pressure: sites distant from GME.

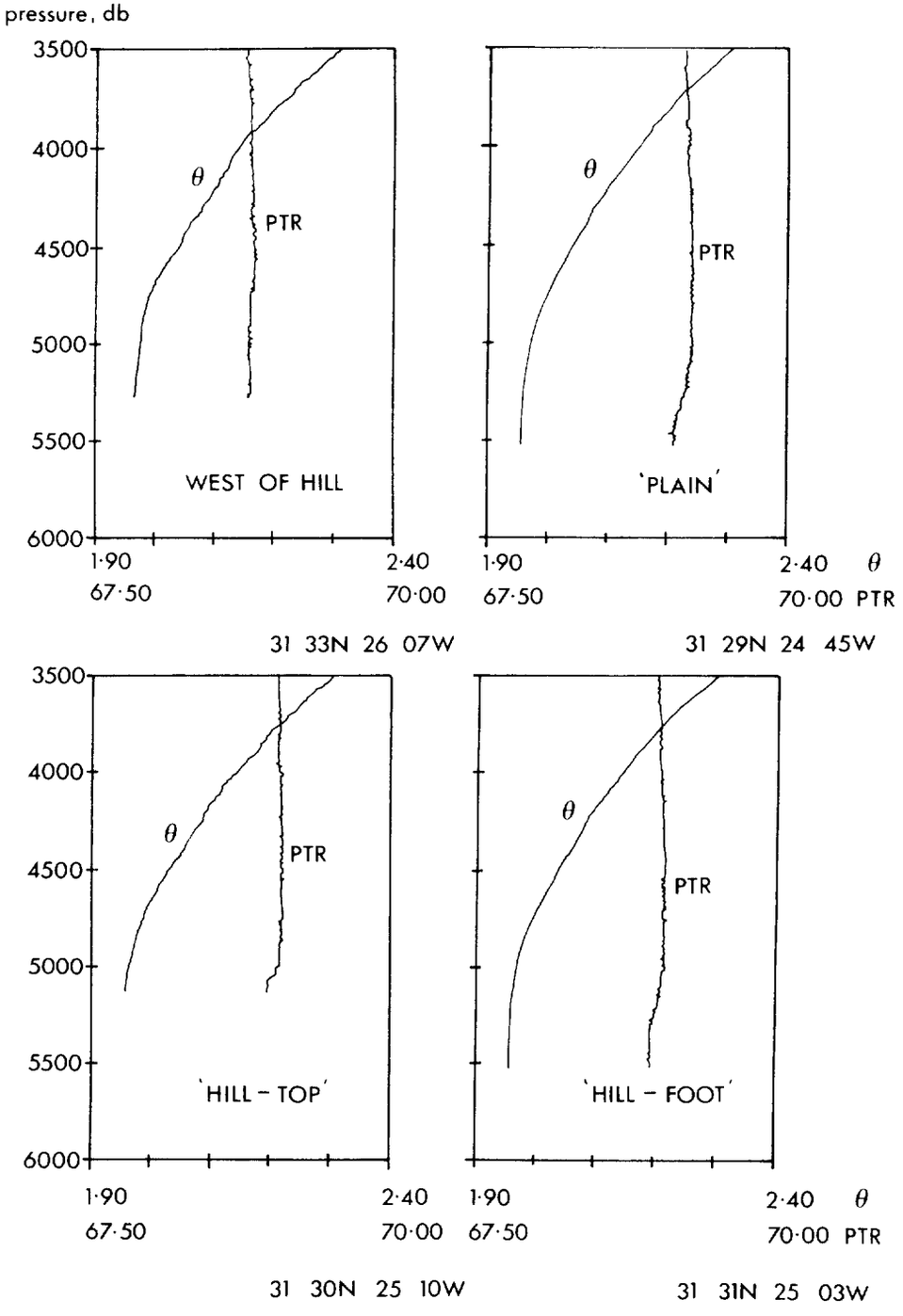

Figure 17 Near bottom profiles of potential transmittance (also temperature) versus pressure: GME study site.

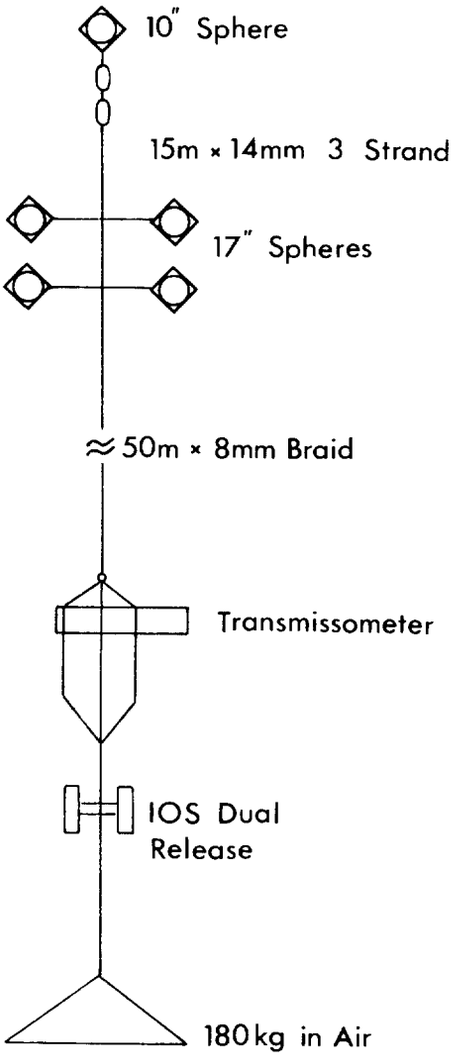

Figure 18 Schematic of transmissometer mooring.

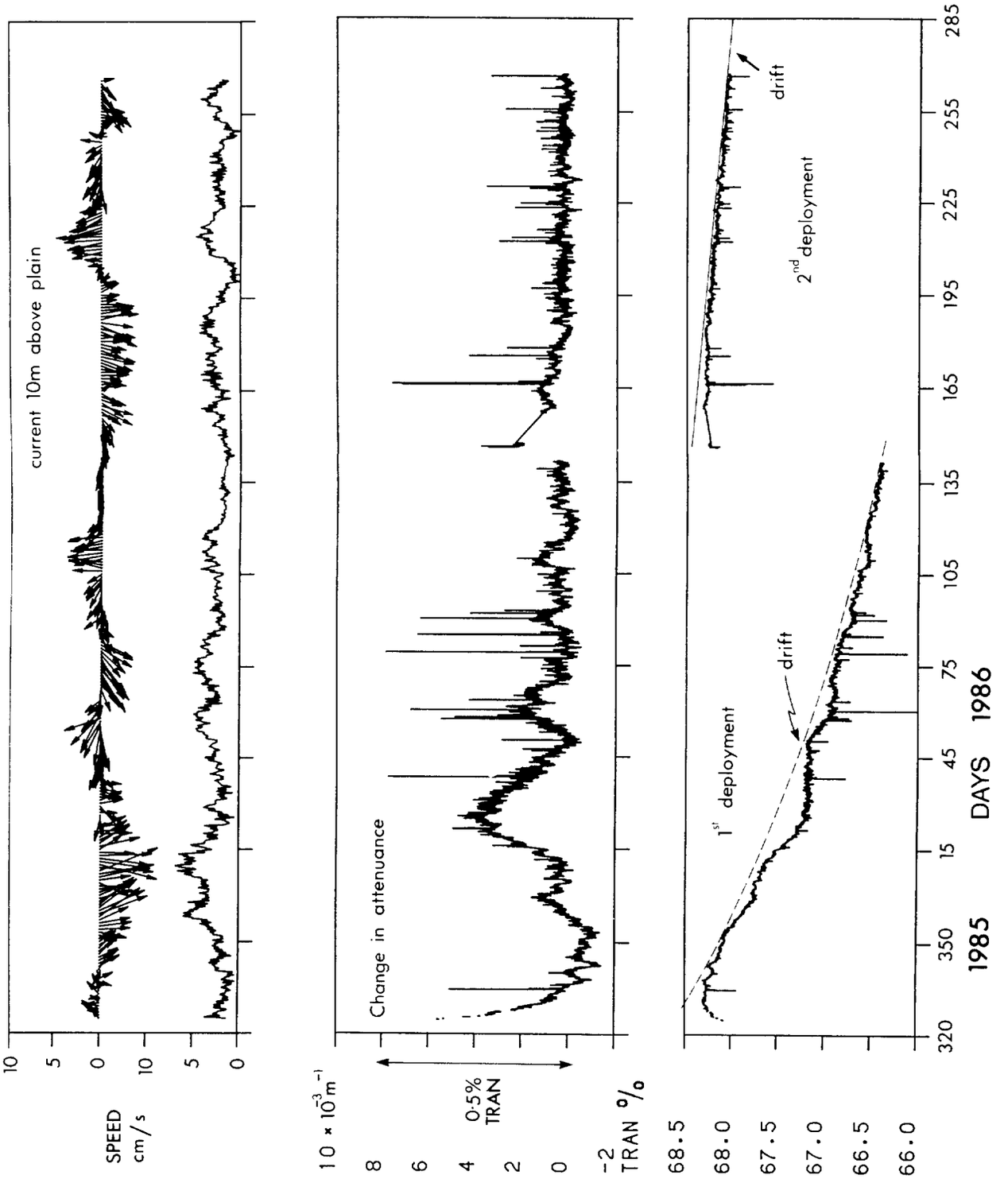

Figure 19 Measurements of currents (10m) and light transmission (3m) on the plain. Lower panel - raw data; centre panel - differences from assumed smooth drift in instrument sensitivity.

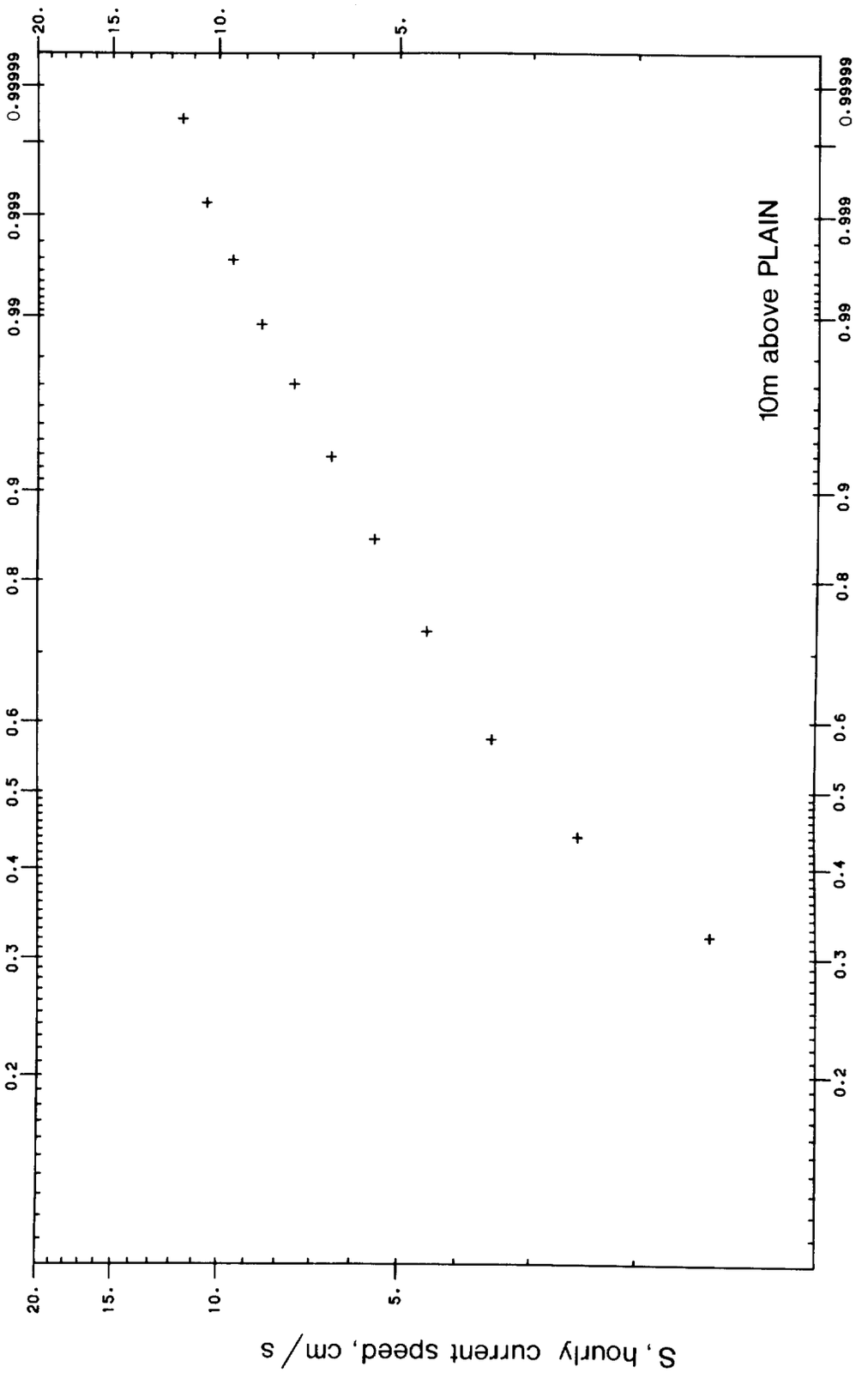

Figure 20 Probability of current speed 10m above sea-bed less than a specified value. The plot linearises a Weibull distribution: PLAIN.

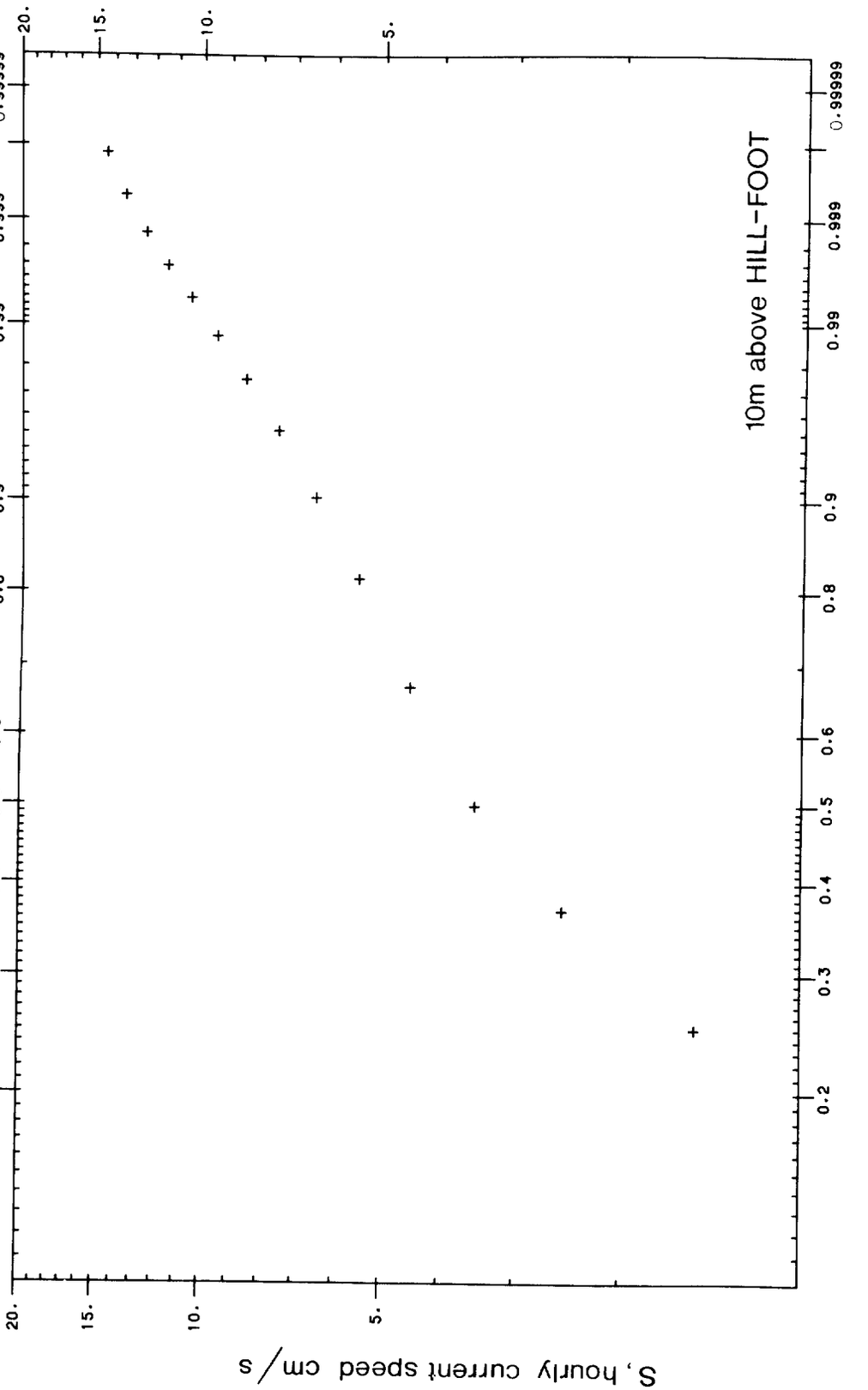

Figure 21 Probability of current speed 10m above sea-bed less than a specified value. The plot linearises a Weibull distribution: HILL-FOOT.

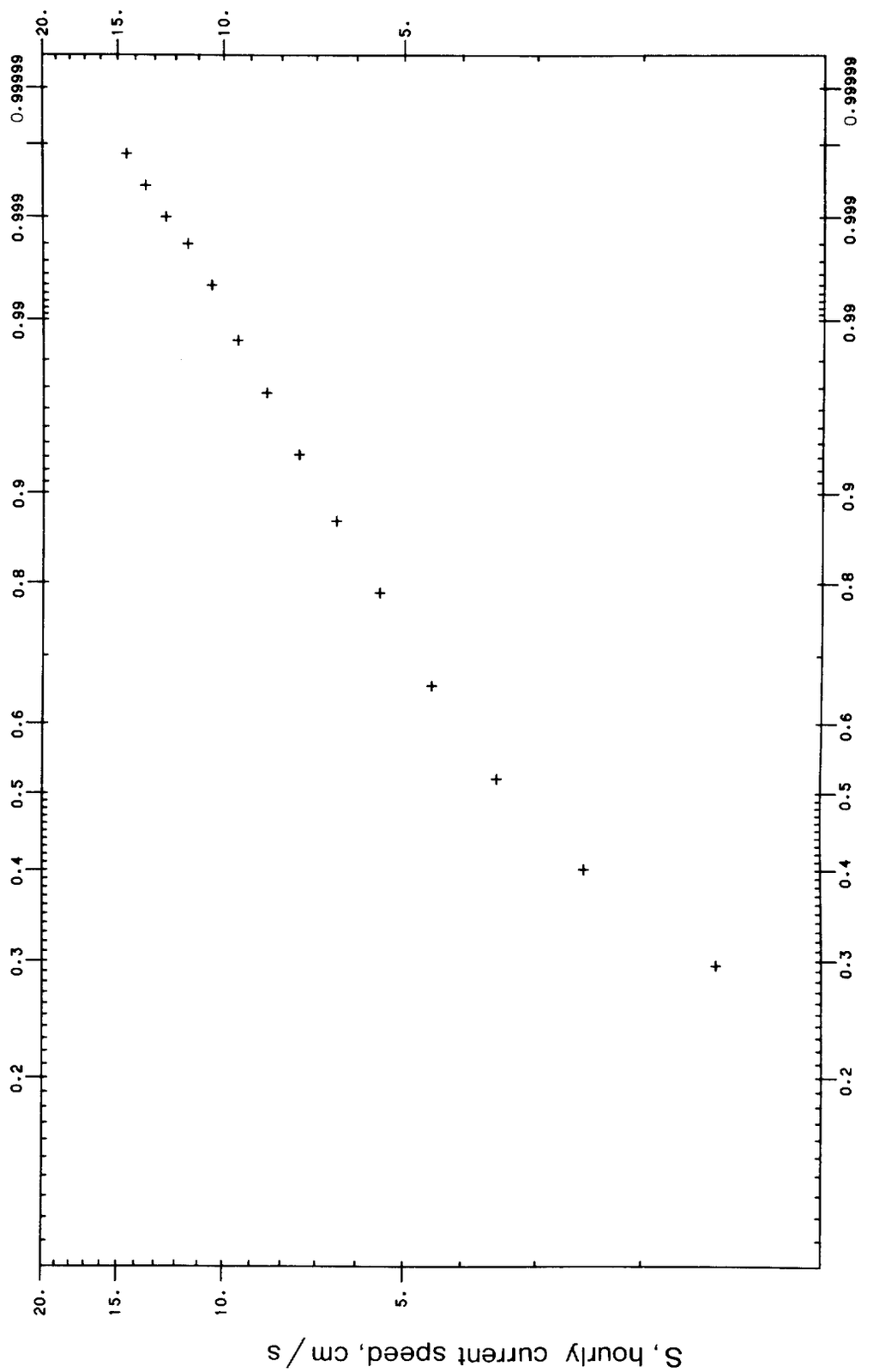

Figure 22 Probability of current speed 10m above sea-bed less than a specified value. The plot linearises a Weibull distribution: HILL-TOP.

RADIOACTIVE WASTE MANAGEMENT

Research Programme 1985/87

DoE Report No.: DoE/RW/87.052

Contract Title: Studies of large and local scale advection and dispersion relevant to the Great Meteor East location.

DoE Reference: PECO7/9/216

Report Title: Currents, dispersion and light transmittance measurements on the Madeira abyssal plain.

Author: P. M. Saunders

Date of submission to DoE: 31.3.87

Period covered covered by Report: 1.4.84 to 31.3.87

Abstract

Near bottom currents have been measured in the GME study area (near 31 30N 25W) over a 3 year period. The sites selected were on top of a small abyssal hill, on its flank and 30km distant from it on the abyssal plain. The magnitude of the mean currents 10m above the sea-bed at the three sites was 1-2 cm/s but their directions were quite different reflecting the presence of a clockwise vortex trapped over the hill. On the plain the mean flow direction was to the west and directly opposed to that furnished by an analysis of the density field.

The variability of the currents is examined: for periods greater than 120 days the variance is concentrated in the east component, and for periods 50-120 days the variance is concentrated in the north component. Current fluctuations propogate westward at speeds 1-10 cm/s but are more complex than barotropic planetary waves. From estimates of the integral time scale of these motions (6-14 days) horizontal diffusivities of between 2 and 5 x 10^2 m^2s^{-1} have been deduced.

Light transmittance measurements have been made from lowerings within the Canary basin and evidence for resuspended sediment is found at most sites. The standing crop of resuspended sediment is quite small, only 1-2gm m^{-2}, about equal to one years accumulation of sediment. Measurements of light transmittance were also made for about 1 year 3m above the bottom at the GME study site: fluctuations were small, corresponded to a particle concentration increase of only a factor of 3, and were uncorrelated with current speeds.

Currents in excess of 10 cm/s occurred infrequently on the plain (about 0.3% of the time) but four times as frequently on and around the hill. Estimates of the highest speeds achieved on average every 50 years have been derived and found less than 20 cm/s. This value is a conservative estimate of the critical speed required to erode the sediment. Thus very infrequent erosion arund GME and especially on the hills can not be excluded: more probable is the advection of sediment from distant sites on the margins where bottom currents are measured to exceed this threshold.

Keywords: 299, 93, 94, 126, 155. DoE sponsored research, Disposal on/under deep ocean bed, Ocean circulation/dispersal, Aquatic dispersion.

This work has been commissioned by the Department of the Environment as part of its radioactive waste management research programme. The results will be used in the formulation of Government policy, but at this stage they do not necessarily represent Government policy.